counterstained with Mayer's hematoxylin, dehydrated, cleared, and mounted with resinous mounting medium. All procedures were performed using AutoStainer (Dako).

2.10. TMA Immunohistochemistry scoring

The optimized staining condition for breast tumor tissue microarray was determined based on the coexistence of both positive and negative cells in the same tissue sample. Signals were considered positive when reaction products were localized in the expected cellular component. The criteria for the staining were scored as follows: distribution score was scored as 0 (0%), 1 (1–50%), and 2 (51–100%) to indicate the percentage of positive cells in all tumor cells present in one tissue. The intensity of the signal (intensity score) was scored as 0 (no signal), 1 (weak), 2 (moderate) or 3 (marked). The total of the distribution score and intensity score was then summed into a total score (TS) of TS0 (sum = 0), TS1 (sum = 2), TS2 (sum = 3), and TS3 (sum = 4–5). Throughout this study, TS0 or TS1 was regarded as negative, whereas TS2 or TS3 was regarded as positive. Statview software was used in statistical analysis.

3. Results

3.1. Optimization of panning methods

To establish a method for the efficient isolation of antibodies against a small amount of protein antigen (nanogram-order or less) prepared from 2D-DIGE spots, 5000 ng, 50 ng or 0.5 ng of recombinant KDR proteins were first immobilized on a BIAcore sensor chip CM3® or on a nitrocellulose membrane using the Bio-Dot Microfiltration Apparatus®. Isolation of antibodies was assessed using a model phage library (anti-KDR scFv antibody-expressing phages: wild type phage = 1: 100) (Fig. 1). Enrichment of the desired clones in the output library was evaluated by analyzing the gene inserts of randomly-picked phage-infected TG1 cells by colony direct PCR. In the method using BIAcore®, enrichment was observed when 5000 ng of KDR was used for immobilization. By contrast, Membrane-based panning led to the successful enrichment of anti-KDR scFv antibodies from only 0.5 ng of KDR. These results demonstrated that membrane-based panning was suitable for the isolation of antibodies from very small amounts of antigen extracted from 2D-DIGE spot gel pieces.

3.2. 2D-DIGE analysis and identification of differentially expressed proteins

To identify breast tumor-related biomarker proteins and isolate monoclonal antibodies against them, we performed 2D-DIGE using breast cancer cell lines SKBR3 and normal breast cell lines 184A1 (Fig. 2). Quantitative analysis showed that 21 spots displayed increased or decreased expression levels in the cancer cell line compared with the normal cell line. MALDI-TOF/MS analysis of the spots subsequently identified 16 different proteins (Table 1).

3.3. Isolation of antibodies against each 2D-DIGE spot from the non-immune scFv phage library

The amount of protein extracted from the gel pieces ranged from several tens of nanogram to a few micrograms (Table 1). Because the membrane-based panning method facilitates the isolation of antibodies from 0.5 ng of protein (Fig. 1), we reasoned that this method could be used to isolate antibodies from the small amounts of proteins extracted from 2D-DIGE spot gel pieces. Thus a portion of the extracted proteins were immobilized onto nitrocellulose membranes by means of a Bio-Dot Microfiltration Apparatus, and membrane-based panning was performed using the non-immune scFv phage library [22] (Table 2). The results from this panning showed that the output/input ratio of phage titer (titer of the recovered phage library after the panning/titer of phage library before the panning) after the fourth round of panning against all spots increased approximately 20-fold–4000-fold in comparison to that obtained from the first round of panning. This elevated output/input ratio indicated the enrichment of the antigen-binding scFv antibody clones. To isolate monoclonal scFv antibodies to each spot, a total of 60 clones were randomly picked from the 4th panning output phage library and binding of the monoclonal scFv antibody-expressing phages to each antigen was tested by phage ELISA. As a result, several scFv antibody clones binding to each of the 16 antigens were isolated (Table 2). The antigenic specificity of isolated scFv antibodies was investigated by dot blot using various proteins as antigens. Some of the isolated scFv antibodies bound specifically to the antigen protein, but not to the His-tagged caspase-8, His-tagged importin-β, tumor necrosis factor receptor 1 (TNFR1)-Fc-chimera and KDR-Fc-chimera (data not shown). These results indicated the successful isolation of each spot-specific scFv antibody-expressing phages after only two weeks.

3.4. TMA analysis

The next stage in the process was to select the most valuable breast tumor-related biomarker proteins from a large number of

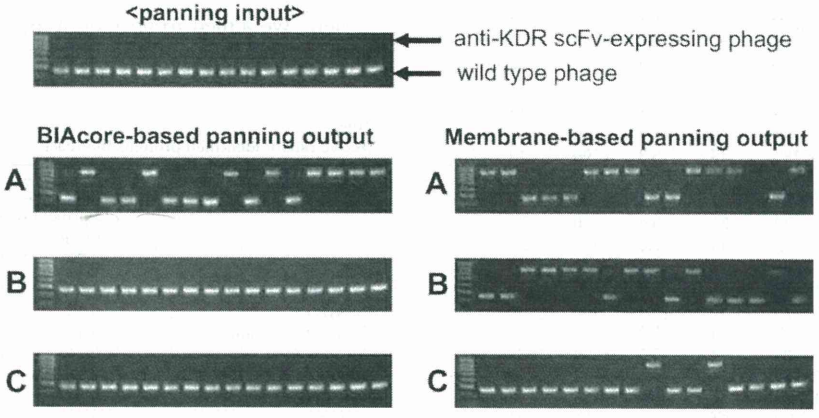

Fig. 1. Optimization of panning methods to isolate monoclonal antibodies from a very small amount of antigen. Model panning was performed using the BIAcore® or nitrocellulose membrane. The model library (anti-KDR scFv phage : wild type phage = 1: 100) was incubated with KDR ((A) 5000 ng, (B) 50 ng, (C) 0.5 ng) immobilized on a sensor chip or nitrocellulose membrane. The BIAcore-based panning method has been previously described [22]. After the binding step, the nitrocellulose membrane was washed ten times with TBST. The bound scFv antibody-expressing phages were eluted with triethylamine. The eluted scFv antibody-expressing phages were then incubated in log phase TG1 cells and individual TG1 clones were picked at random. Inserts of 16 phage clones were amplified by PCR. The gene sizes of inserts were analyzed by agarose gel electrophoresis.

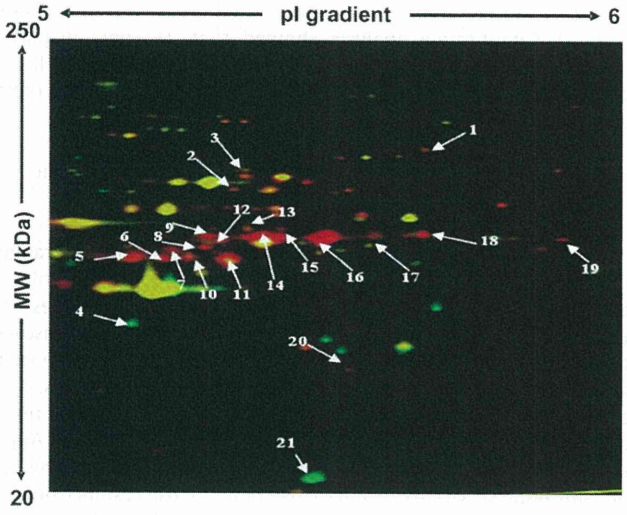

Fig. 2. 2D-DIGE image of fluorescently labeled proteins from SKBR3 and 184A cell. Breast cancer cell line (SKBR3) and normal breast cell line (184A1) were labeled using cy3 and cy5, respectively. The protein samples were then subjected to 2D electrophoresis. Spots that were over- and under-expressed in mammary cancer cells relative to normal cells were colored red and green, respectively. Yellow color spots show no change in expression.

identified candidate proteins. To this end, we immunostained TMA slides with 189 cases of breast tumors and 15 cases of normal breast specimens using the isolated spot-specific scFv antibody-expressing phages and screened the promising candidate biomarker proteins in terms of the expression profile in breast tumor tissues and normal tissues (Table 3). The result of the expression profile analysis showed that SPATA5, beta-actin variant, FLJ31438, PAK65, XRN1 and Jerky protein homolog-like were not expressed in normal and breast cancer tissue at all. By contrast, TRAIL-R2, Cytokeratin 8 and Eph receptor A10 were highly and specifically expressed (Fig. 3) in 63, 73 and 49% of breast tumor cases respectively, while the existing-breast cancer marker, Her-2, was expressed in 28% of breast tumor cases (Table 3). Thus, the relationship between the expression of each antigen and the Her-2 expression profile was analyzed. The level of expression of TRAIL-R2, Cytokeratin 8 and Eph receptor A10 in Her-2 positive cases were 77, 77 and 62%, and in Her-2 negative cases were 57, 67 and 44%, respectively (Table 4). Furthermore, the relationship between the expression of each antigen and clinical stage was analyzed in 187 of the 189 cases where all the clinical data was available. The level of expression of Cytokeratin 8 and Eph receptor A10 increased with progression of clinical symptoms (Table 5).

Table 1
Identification of 2D-DIGE spots by MALDI-TOF/MS.

Spot	Protein name	Accession number	MW (kDa)	pI	Protein volume (ng)	Expression ratio [cancer/normal] (fold)
#1	splicing factor YT521-B	Q96MU7	85	5.9	119	6
#2	IkappaBR	Q96HA7	63	5.5	104	6
#3	SPATA5	C9JT97	76	5.6	94	7
#4	skin aspartic protease	Q53RT3	37	5.3	610	0.1
#5	beta actin variant	P60709	42	5.3	99	15
#6	TRAIL-R2	O14763	48	5.4	100	18
#7	Cytokeratin-18	P05783	48	5.3	99	12
#8	TRAIL-R2	O14763	48	5.4	95	16
#9	RREB1	Q92766	52	5.3	109	10
#10	Cytokeratin-7	P08729	51	5.4	126	23
#11	Cytokeratin-18	P05783	48	5.3	497	13
#12	Cytokeratin-7	P08729	51	5.4	122	24
#13	FLJ31438	Q96N41	53	5.5	126	35
#14	Cytokeratin-7	P08729	51	5.4	406	36
#15	PAK65	Q13177	55	5.7	677	8
#16	Cytokeratin 8	P05787	54	5.5	694	32
#17	Cytokeratin 8	P05787	54	5.5	1143	72
#18	XRN1	Q8IZH2	54	5.8	353	8
#19	Jerky protein homolog-like	Q9Y4A0	51	6.0	130	22
#20	Eph receptor A10	Q5JZY3	32	5.7	119	9
#21	Glutathione S-transferase P	P09211	23	5.4	119	0.02

Table 2
Enrichment and isolation of antibodies to 2D-DIGE spots from non-immune libraries.

Spot	Protein name	Output/Input Ratio ($\times 10^{-7}$)/round				The number of isolated mAb.
		1st	2nd	3rd	4th	
#1	splicing factor YT521-B	6	7	16	480	4
#2	IkappaBR	6	7	15	500	3
#3	SPATA5	5	6	32	860	2
#4	skin aspartic protease	5	6	5	24	1
#5	beta actin variant	7	11	17	480	1
#6	TRAIL-R2	6	7	25	420	5
#7	Cytokeratin 18	5	11	62	260	4
#8	TRAIL-R2	5	27	41	1500	5
#9	RREB1	8	9	14	370	7
#10	Cytokeratin 7	6	7	3	2200	5
#11	Cytokeratin 18	6	8	15	84	2
#12	Cytokeratin 7	10	11	13	94	2
#13	FLJ31438	7	9	32	80	6
#14	Cytokeratin 7	4	7	46	280	5
#15	PAK65	7	11	51	580	9
#16	Cytokeratin 8	8	7	16	4100	6
#17	Cytokeratin 8	5	12	33	240	2
#18	XRN1	6	20	18	200	1
#19	Jerky protein homolog-like	7	10	49	940	3
#20	Eph receptor A10	8	6	57	3000	2
#21	Glutathione S-transferase P	7	8	110	1900	2

4. Discussion

Here, we aimed to develop a method of efficiently screening tumor-related biomarker proteins by proteome analysis. In

Table 3
Positive rate of identified proteins in breast cancer and normal breast tissues.

Protein name	Positive rate of antigens			
	Normal breast tissues		Breast cancer tissues	
Her-2	0/15	(0%)	53/189	(28%)
IkappaBR	3/15	(20%)	22/189	(12%)
SPATA5	0/15	(0%)	0/189	(0%)
beta actin variant	0/15	(0%)	0/189	(0%)
TRAIL-R2	0/15	(0%)	119/189	(63%)
RREB1	1/15	(7%)	83/189	(44%)
FLJ31438	0/15	(0%)	0/189	(0%)
PAK65	0/15	(0%)	0/189	(0%)
Cytokeratin 8	0/15	(0%)	137/189	(73%)
XRN1	0/15	(0%)	0/189	(0%)
Jerky protein homolog-like	0/15	(0%)	0/189	(0%)
Eph receptor A10	0/15	(0%)	93/189	(49%)

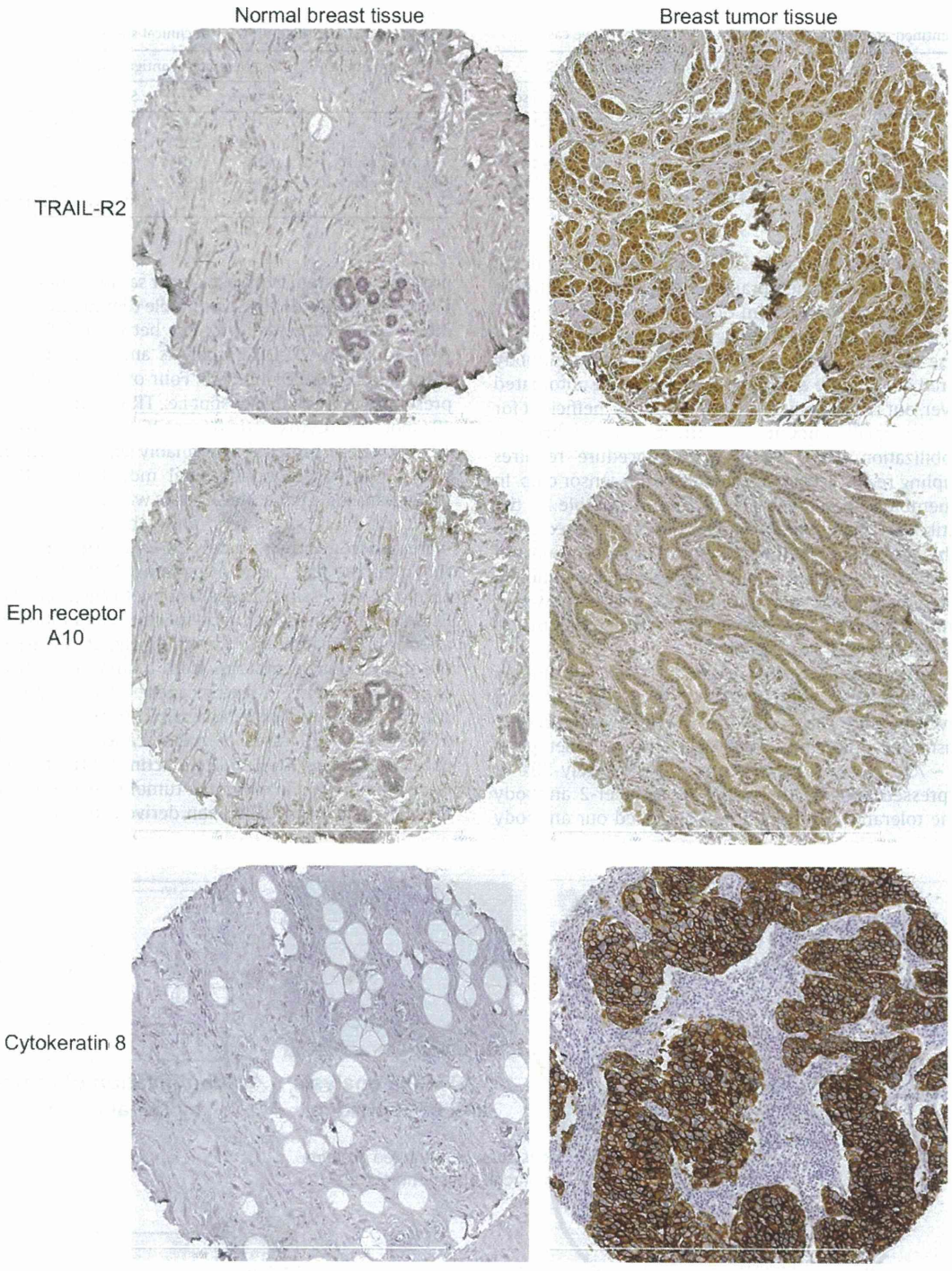

Fig. 3. Immunohistochemical staining of breast tumor and normal breast tissue microarray by scFv antibody-expressing phages. Typical images of breast cancer and normal breast tissue microarray stained by using scFv antibody-expressing phages to TRAIL-R2, Eph receptor A10 and Cytokeratin 8 are shown. Left panels are normal breast tissues and right panels are breast tumors. The tissue microarrays were counterstained by hematoxylin.

particular, we attempted to establish a means of isolating specific antibodies directly from small amounts of differentially expressed proteins obtained *via* 2D-DIGE analysis. To achieve this, we focused on a non-immune scFv phage library. Because the non-immune naïve scFv phage library has a huge repertoire of scFv on the surface of the phages, monoclonal antibodies to every antigen could be effectively isolated *in vitro*. Generally the diversity of the CDR3 domain, which is important for antigen-binding specificity, is estimated to be approximately twenty million [23]. Thus we reasoned that our previously constructed library, containing 2.4×10^9 scFv variants, has almost equal potential as the murine or human immune system [22]. Initially, in order to isolate monoclonal antibodies against very small amounts of antigen (hundreds of nanograms) recovered from the spots of 2D-DIGE analysis, we attempted to optimize the panning method using either a BIAcore® or nitrocellulose membrane. In the method using BIAcore®, the

Table 4
Positive rate of identified proteins in Her-2 positive and Her-2 negative cases.

Protein name	Positive rate of antigens in Her-2	
	Positive cases	Negative cases
TRAIL-R2	41/53 (77%)	78/136 (57%)
Cytokeratin 8	41/53 (77%)	91/136 (67%)
Eph receptor A10	33/53 (62%)	60/136 (44%)
TRAIL-R2 or Eph receptor A10	46/53 (87%)	100/136 (74%)

Table 5
Positive rate of identified proteins in clinical stage.

Protein name	Positive rate of antigens in clinical stage					
	Stage I		Stage II		Stage III	
Her-2	6/14	(43%)	17/87	(20%)	30/86	(35%)
TRAIL-R2	11/14	(79%)	51/87	(59%)	55/86	(64%)
Cytokeratin 8*	7/14	(50%)	58/87	(67%)	71/86	(83%)
Eph receptor A10*	4/14	(29%)	42/87	(48%)	47/86	(55%)
	Man Whitney U test $^*P < 0.05$					

enrichment of the desired clones was observed when immobilizing 5000 ng of KDR. By contrast, membrane-based panning led to the successful enrichment of clones from only 0.5 ng of KDR (Fig. 1). BIAcore-based panning has been recognized to be an effective method because the interaction of an antigen and a scFv antibody can be monitored in real time and the operation can be automated [24,25]. However, our results suggest that BIAcore® is inefficient for immobilizing very small amounts of antigen. This is because antigen immobilization using the BIAcore procedure requires a chemical coupling reaction with the surface of the sensor chip. In contrast, the membrane-based panning method is suitable for the isolation of antibodies against very small amounts of antigens. The suitability of this procedure when handling such small amounts of proteins presumably arises from the high efficiency of adsorption of antigens by the nitrocellulose membrane. These results show that monoclonal antibodies can be created from small amounts of proteins recovered from 2D-DIGE spots.

In breast cancer patients, the antibody targeting human epidermal growth factor receptor II (Her-2), is an effective drug [26,27]. However, because this receptor is over-expressed in only ~25% of breast cancer patients, anti-Her-2 antibody therapy is ineffective in ~75% of cases. Furthemore, approximately 30% of Her-2 over-expressed patients that received anti-Her-2 antibody therapy became tolerant [28–30]. Thus, we applied our antibody proteomics system to breast cancer samples for identification of the proteins to replace Her-2 as suitable therapeutic targets. Initially, 21 differentially expressed proteins between SKBR3 and 184A1 cells were found by 2D-DIGE analysis and 16 different proteins were identified by MALDI-TOF/MS. Four of the identified proteins were present in more than one spot i.e., TRAIL-R2 (spot 6, 8), Cytokeratin 18 (spot 7, 11), Cytokeratin 8 (spot 16, 17) and Cytokeratin 7 (spot 10, 12, 14). These proteins presumably display different pI and MW values due to posttranslational modification. Next, membrane-based panning against these spots was performed, and the output/input ratio of phage titer after the fourth round of panning increased from approximately 20-fold–4000-fold in comparison to that after the first round of panning. Moreover, we screened scFv antibody-expressing phages binding to each spot protein by phage ELISA and obtained each spot-specific scFv antibodies from all spots after approximately two weeks. Finally, it was necessary to select the most valuable proteins from a large number of differentially expressed proteins in breast cancer cells. Using the isolated spot-specific scFv antibody-expressing phages, we immunostained a TMA with 189 cases of breast cancer tissue and 15 samples of normal tissue. SPATA5, Beta actin, FLJ31438, PAK65 and XRN1 were not detected in either the tumor tissue or normal tissue. Thus, these proteins may have been derived from cell lines used in the

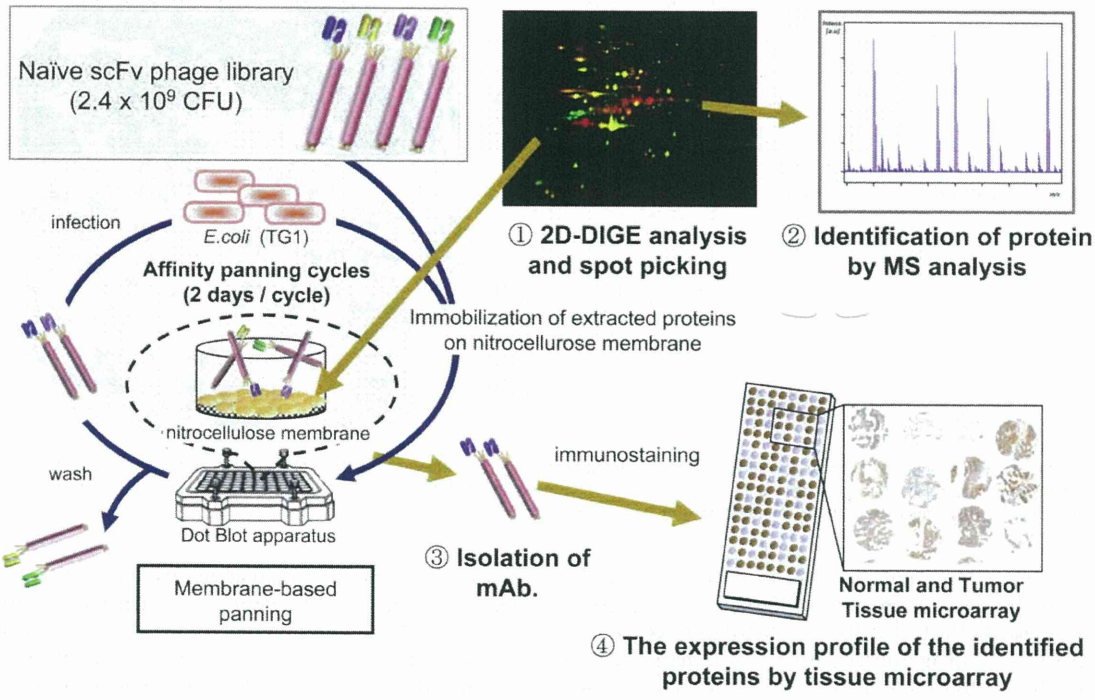

Fig. 4. Schematic illustration of the antibody proteomics system. Antibody proteomics system is an efficient method for screening tumor-related biomarker proteins. Because this system involves the direct isolation of monoclonal antibodies from 2D-DIGE spots without preparation of recombinant proteins, it enables the discovery and validation of tumor-related biomarker proteins by TMA analysis using the isolated scFv antibody-expressing phages.

proteome analysis or the antibodies against these proteins may not detect the antigen on formalin-fixed paraffin-embedded tissues. By contrast, TRAIL-R2, Cytokeratin 8 and Eph receptor A10 were specifically-expressed in over 40% of breast cancer tissues. We confirmed the immunohistochemical staining image generated by scFv antibody-expressing phages displayed a similar pattern to that generated by IgG type commercial antibody (data not shown). Interestingly, the expression rates of TRAIL-R2, Cytokeratin 8 and Eph receptor A10 were higher than the existing breast cancer marker, Her-2 (only about 25%). Moreover, the expression rates of TRAIL-R2 and Eph receptor A10 (cell membrane proteins) in Her-2 negative cases were over 40% and in Her-2 positive cases over 60%. This data indicates that TRAIL-R2 and Eph receptor A10 are promising alternative target candidates for anti-Her-2 antibody therapy ineffective patients, at least in terms of the expression profile. Further work is required to analyze the function of these proteins in more detail. Furthermore, by checking antigen expression profiles against clinical information, the expression rate of Cytokeratin 8 and Eph receptor A10 was found to have increased during progression of the clinical symptoms. These observations indicate that Cytokeratin 8 and Eph receptor A10 are promising diagnostic marker candidates for assessing the aggressiveness of breast cancer.

Recently, an anti-TRAIL-R2 antibody has been developed as an anticancer drug [31–33]. Moreover, Cytokeratin 8 has gained considerable attention as a cancer aggressiveness diagnostic marker [34–36]. These results demonstrate that this technology is able to select well-known drug-target markers (i.e., TRAIL-R2) and diagnostic markers (i.e., Cytokeratin 8) as well as unknown biomarker protein candidates (Eph receptor A10) from a large variety of differentially expressed proteins in cancer cells.

Our method employs a set of techniques for efficiently identifying biomarker candidates. Specifically, the method entails; 1) searching for differentially expressed proteins in disease samples, 2) identification of the proteins, 3) high throughput isolation of monoclonal antibodies against the proteins using a naïve scFv phage library, and 4) validation of the proteins by TMA analysis. This methodology is referred to as an "antibody proteomics system" (Fig. 4). We believe that the proteins identified using this approach will contribute to the drug development process. Indeed, the antibody proteomics system could become a platform technology for seeking tumor-related biomarker proteins by a proteomics-based approach.

5. Conclusions

In this study, we established the antibody proteomics system for efficiently screening and validating tumor-related biomarker proteins of interest by isolating specific antibodies directly from small amounts of proteins obtained *via* 2D-DIGE analysis. Applying this technique to the identification of breast tumor-related biomarker proteins, the expressions of Eph receptor A10, TRAIL-R2 and Cytokeratin 8 in breast tumor tissues were successfully validated from a large number of candidates. These results demonstrate that our original technology is an efficient and useful method for screening tumor-related biomarker proteins. Moreover, Eph receptor A10, TRAIL-R2 and Cytokeratin 8 identified in this study are promising breast tumor biomarkers for drug development.

Acknowledgement

We thank Dr. Junya Fukuoka, Department of Surgical Pathology, Toyama University Hospital, for valuable advice during our pathological analysis.

This study was supported in part by Grants-in-Aid for Scientific Research from the Ministry of Education, Culture, Sports, Science and Technology of Japan, and from the Japan Society for the Promotion of Science (JSPS). This study was also supported in part by Health Labour Sciences Research Grants from the Ministry of Health, Labor and Welfare of Japan, and by Health Sciences Research Grants for Research on Publicly Essential Drugs and Medical Devices from the Japan Health Sciences Foundation.

Appendix

Figure with essential color discrimination. Figs. 2–4 in this article have parts that are difficult to interpret in black and white. The full color images can be found in the on-line version, at doi:10.1016/j.biomaterials.2010.09.030.

References

[1] Hanash S. Disease proteomics. Nature 2003;422(6928):226–32.
[2] Kavallaris M, Marshall GM. Proteomics and disease: opportunities and challenges. Med J Aust 2005;182(11):575–9.
[3] Oh-Ishi M, Maeda T. Disease proteomics of high-molecular-mass proteins by two-dimensional gel electrophoresis with agarose gels in the first dimension (Agarose 2-DE). J Chromatogr B Analyt Technol Biomed Life Sci 2007;849 (1–2):211–22.
[4] Chaga GS. Antibody arrays for determination of relative protein abundances. Methods Mol Biol 2008;441:129–51.
[5] Kaufmann H, Bailey JE, Fussenegger M. Use of antibodies for detection of phosphorylated proteins separated by two-dimensional gel electrophoresis. Proteomics 2001;1(2):194–9.
[6] Xu ZW, Zhang T, Song CJ, Li Q, Zhuang R, Yang K, et al. Application of sandwich ELISA for detecting tag fusion proteins in high throughput. Appl Microbiol Biotechnol 2008;81(1):183–9.
[7] Au NH, Gown AM, Cheang M, Huntsman D, Yorida E, Elliott WM, et al. P63 expression in lung carcinoma: a tissue microarray study of 408 cases. Appl Immunohistochem Mol Morphol 2004;12(3):240–7.
[8] de Jong D, Xie W, Rosenwald A, Chhanabhai M, Gaulard P, Klapper W, et al. Immunohistochemical prognostic markers in diffuse large B-cell lymphoma: validation of tissue microarray as a prerequisite for broad clinical applications (a study from the Lunenburg Lymphoma Biomarker Consortium). J Clin Pathol 2009;62(2):128–38.
[9] Kozarova A, Petrinac S, Ali A, Hudson JW. Array of informatics: applications in modern research. J Proteome Res 2006;5(5):1051–9.
[10] Rimm DL, Camp RL, Charette LA, Costa J, Olsen DA, Reiss M. Tissue microarray: a new technology for amplification of tissue resources. Cancer J 2001;7 (1):24–31.
[11] Tawfik El-Mansi M, Williams AR. Validation of tissue microarray technology using cervical adenocarcinoma and its precursors as a model system. Int J Gynecol Cancer 2006;16(3):1225–33.
[12] Asadi A, Pourfathollah AA, Mahdavi M, Eftekharian MM, Moazzeni SM. Preparation of antibody against horseradish peroxidase using hybridoma technology. Hum Antibodies 2008;17(3–4):73–8.
[13] Hadas E, Theilen G. Production of monoclonal antibodies. The effect of hybridoma concentration on the yield of antibody-producing clones. J Immunol Methods 1987;96(1):3–6.
[14] Makonkawkeyoon L, Pharephan S, Makonkawkeyoon S. Production of a mouse hybridoma secreting monoclonal antibody highly specific to hemoglobin Bart's (gamma4). Lab Hematol 2006;12(4):193–200.
[15] McKinney KL, Dilwith R, Belfort G. Optimizing antibody production in batch hybridoma cell culture. J Biotechnol 1995;40(1):31–48.
[16] Barbas 3rd CF, Kang AS, Lerner RA, Benkovic SJ. Assembly of combinatorial antibody libraries on phage surfaces: the gene III site. Proc Natl Acad Sci U S A 1991;88(18):7978–82.
[17] Coomber DW. Panning of antibody phage-display libraries. Standard protocols. Methods Mol Biol 2002;178:133–45.
[18] McCafferty J, Griffiths AD, Winter G, Chiswell DJ. Phage antibodies: filamentous phage displaying antibody variable domains. Nature 1990;348 (6301):552–4.
[19] Okamoto T, Mukai Y, Yoshioka Y, Shibata H, Kawamura M, Yamamoto Y, et al. Optimal construction of non-immune scFv phage display libraries from mouse bone marrow and spleen established to select specific scFvs efficiently binding to antigen. Biochem Biophys Res Commun 2004;323 (2):583–91.
[20] Smith GP. Filamentous fusion phage: novel expression vectors that display cloned antigens on the virion surface. Science 1985;228(4705):1315–7.
[21] Vaughan TJ, Williams AJ, Pritchard K, Osbourn JK, Pope AR, Earnshaw JC, et al. Human antibodies with sub-nanomolar affinities isolated from a large non-immunized phage display library. Nat Biotechnol 1996;14(3):309–14.

[22] Imai S, Mukai Y, Nagano K, Shibata H, Sugita T, Abe Y, et al. Quality enhancement of the non-immune phage scFv library to isolate effective antibodies. Biol Pharm Bull 2006;29(7):1325–30.
[23] Xu JL, Davis MM. Diversity in the CDR3 region of V(H) is sufficient for most antibody specificities. Immunity 2000;13(1):37–45.
[24] Schier R, Marks JD. Efficient in vitro affinity maturation of phage antibodies using BIAcore guided selections. Hum Antibodies Hybridomas 1996;7 (3):97–105.
[25] Sheets MD, Amersdorfer P, Finnern R, Sargent P, Lindquist E, Schier R, et al. Efficient construction of a large nonimmune phage antibody library: the production of high-affinity human single-chain antibodies to protein antigens. Proc Natl Acad Sci U S A 1998;95(11):6157–62.
[26] Baselga J, Norton L, Albanell J, Kim YM, Mendelsohn J. Recombinant humanized anti-HER2 antibody (Herceptin) enhances the antitumor activity of paclitaxel and doxorubicin against HER2/neu overexpressing human breast cancer xenografts. Cancer Res 1998;58(13):2825–31.
[27] Pietras RJ, Pegram MD, Finn RS, Maneval DA, Slamon DJ. Remission of human breast cancer xenografts on therapy with humanized monoclonal antibody to HER-2 receptor and DNA-reactive drugs. Oncogene 1998;17(17):2235–49.
[28] Amar S, Moreno-Aspitia A, Perez EA. Issues and controversies in the treatment of HER2 positive metastatic breast cancer. Breast Cancer Res Treat 2008;109(1):1–7.
[29] Nahta R, Esteva FJ. In vitro effects of trastuzumab and vinorelbine in trastuzumab-resistant breast cancer cells. Cancer Chemother Pharmacol 2004;53 (2):186–90.
[30] Nahta R, Yu D, Hung MC, Hortobagyi GN, Esteva FJ. Mechanisms of disease: understanding resistance to HER2-targeted therapy in human breast cancer. Nat Clin Pract Oncol 2006;3(5):269–80.
[31] Plummer R, Attard G, Pacey S, Li L, Razak A, Perrett R, et al. Phase 1 and pharmacokinetic study of lexatumumab in patients with advanced cancers. Clin Cancer Res 2007;13(20):6187–94.
[32] Tolcher AW, Mita M, Meropol NJ, von Mehren M, Patnaik A, Padavic K, et al. Phase I pharmacokinetic and biologic correlative study of mapatumumab, a fully human monoclonal antibody with agonist activity to tumor necrosis factor-related apoptosis-inducing ligand receptor-1. J Clin Oncol 2007;25 (11):1390–5.
[33] Vannucchi S, Chiantore MV, Fiorucci G, Percario ZA, Leone S, Affabris E, et al. TRAIL is a key target in S-phase slowing-dependent apoptosis induced by interferon-beta in cervical carcinoma cells. Oncogene 2005;24(15):2536–46.
[34] Ditzel HJ, Strik MC, Larsen MK, Willis AC, Waseem A, Kejling K, et al. Cancer-associated cleavage of cytokeratin 8/18 heterotypic complexes exposes a neoepitope in human adenocarcinomas. J Biol Chem 2002;277 (24):21712–22.
[35] Fukunaga Y, Bandoh S, Fujita J, Yang Y, Ueda Y, Hojo S, et al. Expression of cytokeratin 8 in lung cancer cell lines and measurement of serum cytokeratin 8 in lung cancer patients. Lung Cancer 2002;38(1):31–8.
[36] Wolff JM, Borchers H, Brehmer Jr B, Brauers A, Jakse G. Cytokeratin 8/18 levels in patients with prostate cancer and benign prostatic hyperplasia. Urol Int 1998;60(3):152–5.

Laboratory of Bio-Functional Molecular Chemistry, Graduate School of Pharmaceutical Sciences, Osaka University, Suita, Osaka, Japan

The safety of a mucosal vaccine using the C-terminal fragment of *Clostridium perfringens* enterotoxin

H. Suzuki *, H. Kakutani *, M. Kondoh, A. Watari, K. Yagi

Received April 3, 2010, accepted April 25, 2010

Drs. Masuo Kondoh and Kiyohito Yagi, Laboratory of Bio-Functional Molecular Chemistry, Graduate School of Pharmaceutical Sciences, Osaka University, Suita, Osaka 565-0871, Japan
masuo@phs.osaka-u.ac.jp and yagi@phs.osaka-u.ac.jp
**H.S. and H.K. equally contributed to this study.*

Pharmazie 65: 766–769 (2010) *doi: 10.1691/ph.2010.0097*

The C-terminal fragment of *Clostridium perfringens* enterotoxin (C-CPE) is a claudin-4 binder. Very recently, we found that nasal immunization of mice with C-CPE-fused antigen activated antigen-specific humoral and mucosal immune responses and that the deletion of the claudin-4-binding domain attenuated the immune responses. C-CPE-fusion strategy may be useful for mucosal vaccination. C-CPE is a fragment of enterotoxin, and the safety of C-CPE-fused protein is very important for its future application. In the present study, we investigated whether C-CPE-fused antigen induces immune responses without mucosal injury by using ovalbumin (OVA) as a model antigen. Immunohistochemical analysis showed that claudin-4 was expressed in epithelial cell sheets bordering the nasal cavity. Nasal immunization with C-CPE-fused OVA dose-dependently elevated the OVA-specific serum IgG titer, which was 1000-fold greater than the titer achieved by immunization with OVA or a mixture of OVA and C-CPE at 5 μg of OVA. Nasal immunization with C-CPE-fused OVA (5 μg of OVA) activated Th1 and Th2 responses. Histological analysis showed no mucosal injury in the nasal cavity or nasal passage. C-CPE-fused OVA exhibited mucosal vaccination without mucosal injury. These findings indicate that claudin-4-targeting using C-CPE can be a potent strategy for mucosal vaccination.

1. Introduction

Vaccination is the most potent therapeutic method to overcome infectious diseases. Vaccines are classified as parenteral or mucosal. Parenteral immunizations activate systemic immune responses, while mucosal immunizations activate both systemic and mucosal immune responses. Parenteral vaccination can activate immune responses against the invaded pathogenic microorganisms and infected cells; in contrast, mucosal vaccination prevents entry of the pathogenic microorganisms and activates immune responses against the infected cells (Kunisawa et al. 2008; Neutra and Kozlowski 2006). Although mucosal immunization is promising, an immune response is not activated by the mucosal administration of antigen alone. Efficient antigen delivery into mucosal associated lymphoid tissue (MALT) is the key technology needed for the development of mucosal vaccines (Kunisawa et al. 2008; Neutra and Kozlowski 2006).
The mucosa is covered by epithelial cell sheets, which separate the outside of the body from the inside of the body. Tight junctions (TJs) are located between adjacent epithelial cells and seal intercellular junctions, preventing the free movement of solutes across epithelial cell sheets (Schneeberger and Lynch 1992). Claudin, a tetra-transmembrane protein family consisting of 24 members, plays a pivotal role in the mucosal TJ barrier (Furuse and Tsukita 2006; Tsukita et al. 2001). In 2003, Tamagawa et al. reported that claudin-4 is expressed in the epithelium of intestinal MALT. These findings indicate that claudin-4-targeting may be a novel strategy for the development of mucosal vaccines; however, the claudin-4-targeting vaccine had never been developed because of a delay in the preparation of claudin-4 binder. *Clostridium perfringens* enterotoxin (CPE) causes food poisoning in humans (McClane and Chakrabarti 2004). The CPE receptor is claudin-4, and a 14-kDa polypeptide, the C-terminal fragment of *Clostridium perfringens* enterotoxin (C-CPE), is a claudin-4 binder (Katahira et al. 1997; Sonoda et al. 1999). We previously found that C-CPE enhanced jejunal, nasal and pulmonary absorption of drugs through its interaction with claudin-4 (Kondoh et al. 2005; Uchida et al. 2010). C-CPE is used as a claudin-4 ligand molecule for proteins (Ebihara et al. 2006; Saeki et al. 2009). These findings strongly indicate that C-CPE may be a potent ligand for MALT. Very recently, we have found that intranasal administration of C-CPE-fused ovalbumin (OVA) increased OVA-specific immune-responses in serum, nasal, vaginal and intestinal mucosa (Kakutani et al. 2010). However, C-CPE is a fragment of enterotoxin, and the safety of C-CPE-fused vaccine has never been investigated.
In the present study, we investigated whether nasal immunization with C-CPE-fused OVA activated immune responses without mucosal injury, and we found that mucosal vaccine using C-CPE activated Th1 and Th2 immune responses without nasal mucosa injury.

2. Investigations and results

C-CPE is a binder of claudin-4, and we recently found that claudin-4-targeting using C-CPE might be a potent strategy for mucosal vaccine (Kakutani et al. 2010). C-CPE is a fragment

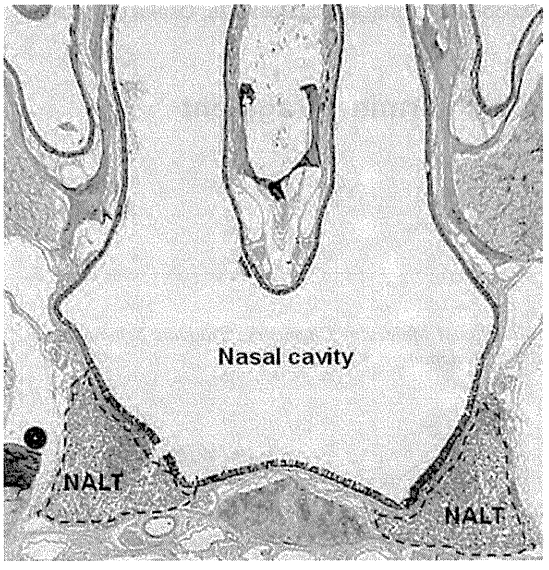

Fig. 1: Immunohistochemical analysis of claudin-4 in NALT Specimens were cryosectioned (4 μm) and stained with anti-claudin-4 Ab, followed by horseradish peroxidase-labeled secondary Ab. The immunoreactive regions were stained with a commercially available staining kit. The regions surrounded by dotted lines are NALT

of CPE (Katahira et al. 1997). CPE is a 35-kDa single polypeptide toxin produced by *Clostridium perfringens*. Experimental and epidemiologic evidence indicates that CPE causes foodborne disease and non-foodborne diarrheal illnesses (McClane 2001; McClane et al. 2000). CPE forms a CPE-containing complex in the plasma membrane that creates massive alterations in plasma membrane permeability that lead to cell death and histological damage to the intestine (McClane and Chakrabarti 2004). The safety of C-CPE is a critical issue for pharmaceutical applications of C-CPE. First, we investigated the expression of claudin-4 in nasal mucosa. Immunohistochemical analysis reveals that claudin-4 is expressed in the epithelium bordering the nasal cavity (Fig. 1). The epithelium that covers nasal MALT, nasopharynx-associated lymphoid tissue (NALT), is rich in claudin-4. These data correspond to our previous data on the expression of claudin-4 mRNA and protein in NALT (Kakutani et al. 2010).

To investigate the dose dependency of OVA-C-CPE in mucosal vaccination, mice were nasally immunized with OVA-C-CPE at 0.5, 1.0 or 5.0 μg of OVA. As shown in Fig. 2A, OVA-specific serum IgG levels were elevated in a dose-dependent manner and reached a level that was 1000-fold greater than the OVA values at 5 μg of OVA, which is the maximal dose of OVA-C-CPE due to its solubility. A mixture of OVA and C-CPE did not increase OVA-specific serum IgG levels (Fig. 2B), and OVA-C-CPE (5.0 μg of OVA) immunization activated IgG2a (a Th1 immune response) and IgG1 (a Th2 immune response) responses (Fig. 2C). We performed a histopathological analysis of mice immunized with OVA-C-CPE at 5.0 μg of OVA. Hematoxylin and eosin (HE) staining revealed no apparent mucosal injury in the nasal squamous cavity, the respiratory cavity, and the nasal passage (Fig. 3A). There was also no inflammatory cell infiltration in the nasal mucosa (Fig. 3B). These findings indicate that nasal immunization with OVA-C-CPE activated immune responses without histological injury in nasal mucosa.

3. Discussion

Only a mucosal vaccine can prevent the entry of pathological viruses into the mucosal membrane; however, injectable vaccines are currently used in both developing and industrialized countries. Very recently, we found that claudin-4-targeting using C-CPE can be a novel strategy for mucosal vaccination (Kakutani et al. 2010). In the present study, we showed that nasal immunization with C-CPE-fused antigen activated Th1 and Th2 immune responses without histological injury in nasal mucosa. The efficient delivery of C-CPE-fused antigen to immunocompetent cells is critical for mucosal vaccination. A mixture of OVA and C-CPE did not activate immune responses, and therefore OVA may be delivered to the immunocompetent cells as the C-CPE-fused protein. The uptake of nasally administered antigens is achieved through a unique set of antigen-sampling cells, the M cells, located in follicle-associated epithelium. After the uptake of antigens by M cells, the antigens are immediately processed and presented to the underlying dendritic cells (Neutra and Kozlowski 2006). A recent report indicates that claudin-4 is expressed in M cells (Rajapaksa et al. 2010). Claudin-4 contains sorting signal sequences to endosomes, an ALGVLL motif at amino acids 92 to 97 and a YVGW motif at amino acids 165 to 168 (Ivanov et al. 2004). These findings suggest that OVA-C-CPE may be taken up by clathrin-mediated endocytosis in

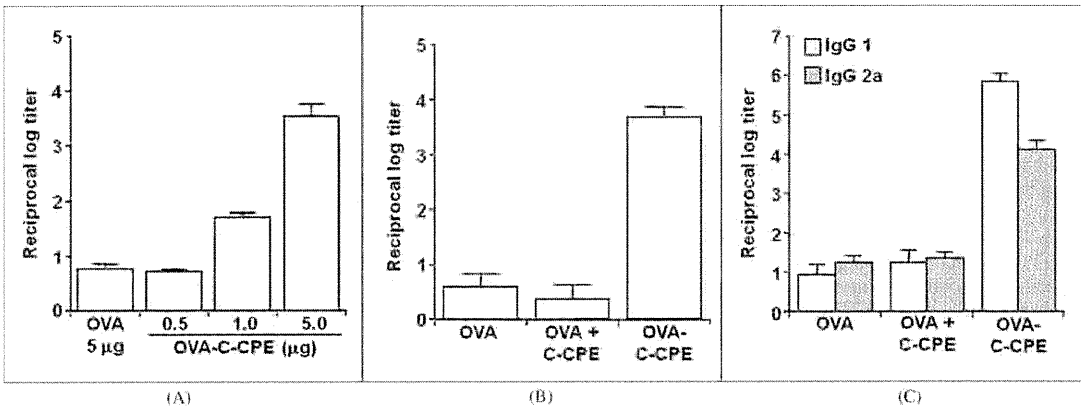

Fig. 2: Production of OVA-specific serum IgG by nasal immunization with OVA-C-CPE Mice were nasally immunized with OVA (5 μg), a mixture of OVA (5 μg) with C-CPE or OVA-C-CPE at the indicated dose of OVA once a week for 3 weeks. Seven days after the last immunization, the serum IgG level was determined by ELISA (A). Mice were nasally immunized with OVA, a mixture of OVA with C-CPE or OVA-C-CPE at 5 μg of OVA once a week for 3 weeks. Seven days after the last immunization, the serum IgG (B), IgG1 and IgG2a (C) levels were determined by ELISA. Data are means ± SEM (n = 4)

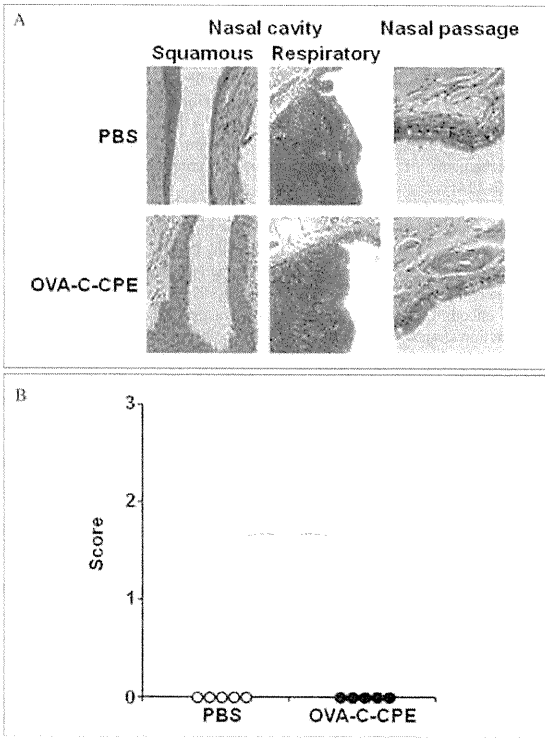

Fig. 3: A lack of histological injury caused by OVA-C-CPE Mice were nasally immunized with PBS or OVA-C-CPE (5 μg OVA) once a week for 3 weeks. Seven days after the last immunization, NALT was collected and fixed with formalin. Thin tissue-sections were stained with hematoxylin (A), and inflammation was scored according to the severity of the inflammatory cell infiltration (B): 0, none; 1, weak; 2, moderate; 3, severe. Scoring was performed blindly to avoid bias

M cells. The underlying mechanism for immunopotentiation by OVA-C-CPE must be clarified.

Nasal mucosa is adjacent to the central nervous system, and intranasal drug delivery to the brain has been developed (Dhuria et al. 2010). An influx of a vaccine protein into the central nervous system can be a risk factor in its clinical application. C-CPE is a modulator of the epithelial barrier. Treatment of nasal mucosa with C-CPE increased the nasal absorption of a peptide drug. OVA-C-CPE also modulated the epithelial barrier *in vitro* (data not shown). Claudin-deficient mice showed a size-dependent leak of solutes smaller than 1,000 Da in the epithelium and endothelium (Furuse et al. 2002; Nitta et al. 2003). C-CPE enhanced the mucosal absorption of dextran with a molecular mass of ~20 kDa (Kondoh et al. 2005). Because OVA-C-CPE has a molecular mass of 65 kDa, and the infiltration of inflammatory lymphocytes was not observed in nasal mucosa (Fig. 3B), OVA-C-CPE might not cause an influx of solutes across the nasal epithelium. The claudin family comprises at least 24 members. Interestingly, the barrier-function and expression profiles of claudin family members differ among tissues. Claudin is believed to form homophilic and heterophilic adhesions in TJ strands, and various combinations of the 24 family members are thought to create diversity in the structure and functions of TJ barriers (Furuse and Tsukita 2006; Morita et al. 1999; Tsukita et al. 2001). Targeting the type of claudin specifically expressed in NALT may reduce the risk of delivering solutes to the central nervous system.

In summary, we showed that nasal immunization with C-CPE-fused antigen activated Th1 and Th2 immune responses without mucosal injury. This is the first report to indicate the safety of a claudin-4-targeting mucosal vaccine using C-CPE. Future improvement of the claudin specificity may lead to clinical applications of this type of vaccine.

4. Experimental

4.1. Animals

Female BALB/c mice were purchased from SLC, Inc. (Shizuoka, Japan). The mice were housed at 23 ± 1.5 °C with a 12-h light/dark cycle and had free access to standard rodent chow and water. The protocol of this study was approved by the Animal Care and Use Committee for Graduate School of Pharmaceutical Sciences, Osaka University.

4.2. Immunohistochemical analysis

Immunohistochemical staining for claudin-4 was performed with an autostainer (Dako, Glostrup, Denmark). Slide-mounted, fixed cryosections (4-μm thick) of nasal MALT were incubated in Dako target retrieval solution (pH 9) at 125 °C for 30 min and then 90 °C for 10 min. The slides were blocked with peroxidase-blocking reagent (Dako) for 5 min and then with 10% bovine serum albumin for 30 min. The slides were further incubated with anti-claudin-4 antibody followed by horseradish peroxidase-labeled secondary antibody. The immunoreactive proteins were stained with DAB substrate (Dako). The slides were also stained with hematoxylin solution. Tissue sections were observed under a microscope.

4.3. Preparation of C-CPE-fused OVA

C-CPE-fused OVA (OVA-C-CPE) was prepared as described previously (Kakutani et al. 2010). Briefly, the plasmid pET-OVA-C-CPE was transduced into *Escherichia coli* BL21 (DE3), and the production of OVA-C-CPE was stimulated with isopropyl-D-thiogalactopyranoside. The harvested cells were lysed in buffer A (10 mM Tris-HCl, pH 8.0, 400 mM NaCl, 5 mM $MgCl_2$, 0.1 mM phenylmethylsulfonyl fluoride, 1 mM 2-mercaptoethanol, and 10% glycerol). The lysates were applied to HiTrap™ Chelating HP (GE Healthcare UK Ltd., Buckinghamshire, UK), and OVA-C-CPEs were eluted with buffer A containing 100-400 mM imidazole. The buffer was exchanged with phosphate-buffered saline (PBS) by using a PD-10 column (GE Healthcare UK Ltd.), and the purified protein was stored at −80 °C before use. Purification of the OVA-C-CPEs was confirmed by sodium dodecyl sulfate-polyacrylamide gel electrophoresis, followed by staining with Coomassie Brilliant Blue. Protein was quantified by using a BCA protein assay kit (Pierce Chemical, Rockford, IL) with BSA as a standard.

4.4. Nasal immunization and sample collection

Mice were nasally immunized once a week for 3 weeks at the indicated dose of OVA. For instance, a dose of 5 μg OVA is equal to a mixture of OVA (5 μg) and C-CPE (1.89 μg) or OVA-C-CPE (6.89 μg). Plasma was collected 7 days after the last nasal immunization.

4.5. OVA-specific IgG production

The titers of OVA-specific antibody in serum were determined by enzyme-linked immunosorbent assay (ELISA). Briefly, an immunoplate was coated with OVA (100 μg/well in a 96-well plate). Ten-fold serial dilutions of these samples were added to the immunoplate followed by the addition of horseradish peroxidase-conjugated goat anti-mouse IgG, IgG1 or IgG2a (Bethyl Laboratories Inc., Montgomery, TX). The OVA-specific antibodies were detected by using a TMB peroxide substrate (Thermo Fisher Scientific Inc., Rockford, IL). End-point titers were expressed as the reciprocal log of the last dilution ratio, which was 0.1 greater than the control values obtained for the serum of naïve mice at an absorbance of 450 nm.

4.6. Histological analysis of nasal mucosa in mice immunized with OVA-C-CPE

Mice from either the non-immunized group or the immunized group (6.89 μg of OVA-C-CPE) were sacrificed 7 days after immunization for histopathological analysis. Tissues were fixed with 4% paraformaldehyde and embedded in paraffin. Sections (4 μm) were prepared for hematoxylin and eosin staining. Histopathologic examinations were performed at the Applied Medical Research Laboratory (Osaka, Japan). Inflammation was scored according to the severity of the inflammatory cell infiltration: 0, none; 1, weak; 2, moderate; and 3, severe. Scoring was performed blindly to avoid bias.

Acknowledgements: We thank Drs S. Tsunoda and K. Nagano (National Institute of Biomedical Innovation), Y. Horiguchi and S. Nakagawa (Osaka University) for their instructing immunohistochemical analysis, providing C-CPE cDNA and OVA cDNA, respectively. We also thank the all members of our laboratory for their useful comments and discussion. This work was supported by a Grant-in-Aid for Scientific Research from the Ministry of Education, Culture, Sports, Science and Technology, Japan (21689006), by a Health and Labor Sciences Research Grants from the Ministry of Health, Labor and Welfare of Japan, by Takeda Science Foundation, by a grant from Kansai Biomedical Cluster project in Saito, which is promoted by the Knowledge Cluster Initiative of the Ministry of Education, Culture, Sports, Science and Technology, Japan, by a Research Grant for Promoting Technological Seeds from Japan Science and Technology Agency and the Japan Health Sciences Foundation. H.K. is supported by Research Fellowships of the Japan Society for the Promotion of Science for Young Scientists.

References

Dhuria SV, Hanson LR, Frey WH (2010) Intranasal delivery to the central nervous system: mechanisms and experimental considerations. J Pharm Sci 99: 1654–1673.

Ebihara C, Kondoh M, Hasuike N, Harada M, Mizuguchi H, Horiguchi Y, Fujii M, Watanabe Y (2006) Preparation of a claudin-targeting molecule using a C-terminal fragment of *Clostridium perfringens* enterotoxin. J Pharmacol Exp Ther 316: 255–260.

Furuse M, Hata M, Furuse K, Yoshida Y, Haratake A, Sugitani Y, Noda T, Kubo A, Tsukita S (2002) Claudin-based tight junctions are crucial for the mammalian epidermal barrier: a lesson from claudin-1-deficient mice. J Cell Biol 156: 1099–1111.

Furuse M, Tsukita S (2006) Claudins in occluding junctions of humans and flies. Trends Cell Biol 16: 181–188.

Ivanov AI, Nusrat A, Parkos CA (2004) Endocytosis of epithelial apical junctional proteins by a clathrin-mediated pathway into a unique storage compartment. Mol Biol Cell 15: 176–188.

Kakutani H, Kondoh M, Fukasaka M, Suzuki H, Hamakubo T, Yagi K (2010) Mucosal vaccination using claudin-4-targeting. Biomaterials 20: 5463–5471.

Katahira J, Inoue N, Horiguchi Y, Matsuda M, Sugimoto N (1997) Molecular cloning and functional characterization of the receptor for *Clostridium perfringens* enterotoxin. J Cell Biol 136: 1239–1247.

Kondoh M, Masuyama A, Takahashi A, Asano N, Mizuguchi H, Koizumi N, Fujii M, Hayakawa T, Horiguchi Y, Watanbe Y (2005) A novel strategy for the enhancement of drug absorption using a claudin modulator. Mol Pharmacol 67: 749–756.

Kunisawa J, Nochi T, Kiyono H (2008) Immunological commonalities and distinctions between airway and digestive immunity. Trends Immunol 29: 505–513.

McClane BA (2001) *Clostridium perfringens*. In: Doyle MP, Beuchat LR, Montville TJ, editors. Food miclobiology: fundamentals and frontiers. Washington, DC: ASM Press: 352–372.

McClane BA, Chakrabarti G (2004) New insights into the cytotoxic mechanisms of *Clostridium perfringens* enterotoxin. Anaerobe 10: 107–114.

McClane BA, Lyerly DM, Moncrief JS, Wilkins TD (2000) Enterotoxic clostridia: *Clostridium perfringens* type A and *Clostridium difficile*. In: Fischetti VA, Novick RP, Ferretti JJ, Portnoy DA, Rood JI, editors. Gram-positive pathogens. Washington, DC: ASM Press: 551–562.

Morita K, Furuse M, Fujimoto K, Tsukita S (1999) Claudin multigene family encoding four-transmembrane domain protein components of tight junction strands. Proc Natl Acad Sci USA 96: 511–516.

Neutra MR, Kozlowski PA (2006) Mucosal vaccines: the promise and the challenge. Nat Rev Immunol 6: 148–158.

Nitta T, Hata M, Gotoh S, Seo Y, Sasaki H, Hashimoto N, Furuse M, Tsukita S (2003) Size-selective loosening of the blood-brain barrier in claudin-5-deficient mice. J Cell Biol 161: 653–660.

Rajapaksa TE, Stover-Hamer M, Fernandez X, Eckelhoefer HA, Lo DD (2010) Claudin 4-targeted protein incorporated into PLGA nanoparticles can mediate M cell targeted delivery. J Control Release 142: 196–205.

Saeki R, Kondoh M, Kakutani H, Tsunoda S, Mochizuki Y, Hamakubo T, Tsutsumi Y, Horiguchi Y, Yagi K (2009) A novel tumor-targeted therapy using a claudin-4-targeting molecule. Mol Pharmacol 76: 918–926.

Scheneeberger EE, Lynch RD (1992) Structure, function, and regulation of cellular tight junctions. Am J Physiol 262: L647–L661.

Sonoda N, Furuse M, Sasaki H, Yonemura S, Katahira J, Horiguchi Y, Tsukita S (1999) *Clostridium perfringens* enterotoxin fragment removes specific claudins from tight junction strands: Evidence for direct involvement of claudins in tight junction barrier. J Cell Biol 147: 195–204.

Tamagawa H, Takahashi I, Furuse M, Yoshitake-Kitano Y, Tsukita S, Ito T, Matsuda H, Kiyono H (2003) Characteristics of claudin expression in follicle-associated epithelium of Peyer's patches: preferential localization of claudin-4 at the apex of the dome region. Lab Invest 83: 1045–1053.

Tsukita S, Furuse M, Itoh M (2001) Multifunctional strands in tight junctions. Nat Rev Mol Cell Biol 2: 285–293.

Uchida H, Kondoh M, Hanada T, Takahashi A, Hamakubo T, Yagi K (2010) A claudin-4 modulator enhances the mucosal absorption of a biologically active peptide. Biochem Pharmacol 79: 1437–1444.

Hepatoprotective Effect of Syringic Acid and Vanillic Acid on CCl_4-Induced Liver Injury

Ayano ITOH,[a] Katsuhiro ISODA,[a] Masuo KONDOH,[a] Masaya KAWASE,[a] Akihiro WATARI,[a] Masakazu KOBAYASHI,[b] Makoto TAMESADA,[b] and Kiyohito YAGI*,[a]

[a] *Graduate School of Pharmaceutical Sciences, Osaka University; 1–6 Yamada-oka, Suita, Osaka 565–0871, Japan: and* [b] *Research and Development Center, Kobayashi Pharmaceutical Co., Ltd.; 1–30–3 Toyokawa, Ibaraki, Osaka 567–0057, Japan.* Received December 22, 2009; accepted March 16, 2010; published online March 19, 2010

The mycelia of the edible mushroom *Lentinula edodes* can be cultured in solid medium containing lignin, and the hot-water extracts (L.E.M.) is commercially available as a nutritional supplement. During the cultivation, phenolic compounds, such as syringic acid and vanillic acid, were produced by lignin-degrading peroxidase secreted from *L. edodes* mycelia. Since these compounds have radical scavenging activity, we examined their protective effect on oxidative stress in mice with CCl_4-induced liver injury. We examined the hepatoprotective effect of syringic acid and vanillic acid on CCl_4-induced chronic liver injury in mice. The injection of CCl_4 into the peritoneal cavity caused an increase in the serum aspartate aminotransferase (AST) and alanine aminotransferase (ALT) levels. The intravenous administration of syringic acid and vanillic acid significantly decreased the levels of the transaminases. Four weeks of CCl_4 treatment caused a sufficiently excessive deposition of collagen fibrils. An examination of Azan-stained liver sections revealed that syringic acid and vanillic acid obviously suppressed collagen accumulation and significantly decreased the hepatic hydroxyproline content, which is the quantitative marker of fibrosis. Both of these compounds inhibited the activation of cultured hepatic stellate cells, which play a central role in liver fibrogenesis, and maintained hepatocyte viability. These data suggest that the administration of syringic acid and vanillic acid could suppress hepatic fibrosis in chronic liver injury.

Key words hepatoprotection; *Lentinula edodes*; syringic acid; vanillic acid; polyphenol

The edible mushroom *Lentinula edodes* (shiitake) contains bioactive compounds that have immune-modulating, antitumor, antibacterial, antiviral, and antiparasitic effects.[1—4] The mycelia of *L. edodes* can be cultured in solid medium, and the hot-water extract (L.E.M.) is commercially available as a nutritional supplement. The main components of L.E.M. are sugars, proteins, and polyphenolic compounds. Polyphenols have protective effects against cancers, cardiovascular disease, and neurodegenerative disorders.[5—7] Among polyphenols, syringic acid and vanillic acid are enriched in the solid medium of cultured *L. edodes* mycelia.[8] *L. edodes* grown in lignocellulose secretes lignin-degrading peroxidase into the culture medium.[9] The mycelia-derived enzymes degrade the lignin to produce phenolic compounds, particularly syringic acid and vanillic acid. In our previous study, we demonstrated that these phenolic compounds had a hepatoprotective effect on concanavalin A (ConA)-induced liver injury in mice.[8] We intraperitoneally injected syringic acid or vanillic acid into mice shortly before a ConA injection into the tail vein, which greatly increased the levels of serum aspartate aminotransferase (AST) and alanine aminotransferase (ALT). In addition, the inflammatory cytokines tumor necrosis factor (TNF)-α, interferon-γ (IFN-γ), and interleukin (IL)-6 in the serum increased rapidly, within 3 h of the ConA administration. The administration of syringic acid or vanillic acid significantly decreased the transaminase and inflammatory cytokine levels and suppressed the disorganization of the hepatic sinusoids. Since ConA-induced liver injury is a mouse model of immune-mediated liver injury that resembles viral and autoimmune hepatitis in humans, the phenolics appeared to have immunomodulating activity.

Polyphenols act as antioxidants by scavenging reactive oxygen species (ROS), which produce oxidative stress and can adversely affect many cellular processes. In the present study, we examined the possible hepatoprotective effects of two phenolic compounds, syringic acid and vanillic acid, on oxidative stress in chronic CCl_4-induced liver injury in mice. We found that both phenolic compounds could suppress oxidative damage, especially liver fibrosis caused by repeated administration of CCl_4.

MATERIALS AND METHODS

Reagents Syringic acid, vanillic acid, and CCl_4 were purchased from WAKO Pure Chemicals, Co., Ltd. (Osaka, Japan). The chemical structures of syringic acid and vanillic acid were shown in Fig. 1. L.E.M. was obtained from Kobayashi Pharmaceutical Co., Ltd. (Osaka, Japan). CCl_4 was dissolved in olive oil, and L.E.M., syringic acid, and vanillic acid were dissolved in phosphate buffered saline (PBS) for administration into mice. L.E.M., syringic acid, and vanillic acid were dissolved in culture medium for hepatocytes or hepatic stellate cells for *in vitro* experiments.

Animals BALB/c mice and Sprague-Dawley rats were purchased from SLC (Shizuoka, Japan). The animals were housed in an air-conditioned room at 22 °C before the experiment. The animal experiments were conducted according to the ethical guidelines of Osaka University Graduate School

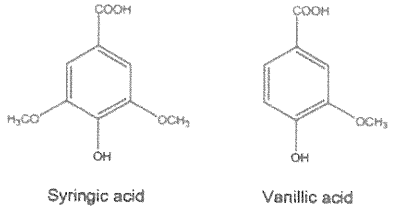

Fig. 1. Chemical Structures of Syringic Acid and Vanillic Acid

* To whom correspondence should be addressed. e-mail: yagi@phs.osaka-u.ac.jp

of Pharmaceutical Sciences. The experimental protocol was submitted to the Committee on the Guidelines for Animal Experiments in Graduate School of Pharmaceutical Sciences, and the experiments were conducted after gaining the approval. Mice in the chronic liver injury model received intraperitoneal injections of CCl_4 (0.5 ml/kg body weight) and intravenously administered L.E.M., syringic acid, or vanillic acid (10 mg/kg body weight) twice a week for 4 weeks. Twenty-four hours after the L.E.M., syringic acid, or vanillic acid injection, the mice were anesthetized. Then, blood samples were collected to determine the transaminase activity, and the livers were excised for Azan staining and determination of hydroxyproline and malondialdehyde.

Assays Serum AST and ALT levels were measured by using an assay kit (Transaminase C-II, WAKO, Osaka, Japan).

Histological Analysis Liver specimens were fixed in 4% paraformaldehyde and embedded in paraffin. Sections were cut from the tissue blocks and mounted on slides. Azan staining was then performed to evaluate the extent of liver fibrosis.

Measurement of Hydroxyproline Content Hepatic hydroxyproline content was measured by using Kivirikko's method[10] with some modifications. Briefly, liver tissue (50 mg) was hydrolyzed with 6 mol/l HCl at 110 °C for 24 h in a glass test tube. After centrifugation at 3000 rpm for 10 min, 2 ml of the supernatant was neutralized with 8 N KOH. Two grams of KCl and 1 ml of 0.5 mol/l borate buffer were then added to the neutralized supernatant, followed by a 15-min incubation at room temperature and then a 15-min incubation at 0 °C. Freshly prepared chloramine-T solution was then added, and the sample was incubated at 0 °C for 1 h, followed by the addition of 2 ml of 3.6 mol/l sodium thiosulfate. The samples were incubated at 120 °C for 30 min. Then, 3 ml of toluene was added, and the samples were incubated for 20 min at room temperature. After centrifugation at 2000 rpm for 5 min, 2 ml of the supernatant was added to 0.8 ml buffer containing Ehrlich's reagent and incubated for 30 min at room temperature. The samples were then transferred to a plastic tube, and the absorbance was measured at 560 nm. The hydroxyproline content was expressed as micrograms of hydroxyproline per gram of liver.

Measurement of Malondialdehyde Lyophilized liver tissue (25 mg) was boiled for 30 min in a solution containing 250 ml of 1.15% KCl, 150 ml of 1% H_3PO_4, and 500 ml of 0.67% thiobarbituric acid. Two milliliters of *n*-butanol was added to the ice-chilled sample, and then the sample was stirred for 30 min. After centrifugation at $3000\times g$ for 10 min, the upper *n*-butanol phase was collected, and the amount of malondialdehyde was colorimetrically determined at 535 and 520 nm.

Isolation and Culture of Hepatic Stellate Cells Hepatic stellate cells (HSCs) were isolated from 10-week-old male Sprague-Dawley rats by digesting the liver with Pronase-E (Merck Darmstadt, Germany) and collagenase type I (WAKO Pure Chemicals Co., Osaka, Japan) as previously described.[11] Isolated HSCs were seeded at a density of 2×10^5 cells/cm^2 onto 24-well polystyrene culture plates (Asahi Techno Glass, Funabashi, Chiba, Japan) to observe the morphology and analyze fibrosis-related gene expression. Cells were cultured in Dulbecco's modified Eagle's medium (Sigma, St. Louis, MO, U.S.A.) supplemented with 10% fetal bovine serum.

Isolation and Culture of Hepatocytes Hepatocytes were isolated from male BALB/c mice by perfusing the liver with collagenase, according to the method of Seglen.[12] Cells were seeded at a density of 1×10^5 cells/cm^2 into multi-well culture plates pre-coated with collagen type I (Asahi Techno Glass, Funabashi, Chiba, Japan). The basal medium consisted of 50 U/ml penicillin G, 50 μg/ml streptomycin (ICN Biochemicals, Inc., Costa Mesa, CA, U.S.A.), 1 μM insulin, 1 μM dexamethasone (WAKO Pure Chemicals Co., Osaka, Japan), and 10% fetal bovine serum in William's medium E (MP Biomedicals, Inc., Kayserberg, France). Six hours after the cells were seeded, the basal medium was replaced with medium containing L.E.M., syringic acid, or vanillic acid at a final concentration of 1.0 mg/ml without insulin and dexamethasone. Cells were then cultured for 24—48 h, and viable cells were counted after trypan blue staining.

Reverse Transcription-Polymerase Chain Reaction (RT-PCR) The HSCs were cultured for 7 d and the total RNA was extracted using High Pure RNA Isolation Kit (Roche, Mannheim, Germany). The gene expression of collagen I α(I) was analyzed using the following primers: forward 5′-TGCCGTGACCTCAAGATGTG-3′ and reverse 5′-CACAAGCGTGCTGTAGGTGA-3′. The gene expression of a smooth muscle actin (α-SMA) was analyzed using the following primers: forward 5′-CCGAGATCTCACCGACTACC-3′ and reverse 5′-TCCAGAGCGACATAGCACAG-3′. The gene expression of β-actin was analyzed using the following primers: forward 5′-CCCAGAGCAAGAGAGGCATC-3′ and reverse 5′-CTCAGGAGGAGCAATGATCT-3′.

The RT-PCR was examined using RNA PDR Kit (TaKaRa, Kyoto, Japan).

Statistical Analysis The data were analyzed for statistical significance by using Student's *t*-test and Dunnett's test.

RESULTS

Effect on CCl_4-Induced Chronic Liver Injury We examined the hepatoprotective effect of syringic acid and vanillic acid on CCl_4-induced chronic liver injury in mice. As shown in Fig. 2, after 4 weeks of CCl_4 treatment, the activities of blood AST and ALT increased 30-fold and 127-fold, respectively, compared with controls. The intravenous administration of syringic acid or vanillic acid significantly decreased the activities of AST and ALT. These results suggest that syringic acid and vanillic acid suppress the hepatic inflammation caused by repeated CCl_4 treatments. We also examined the effect of syringic acid and vanillic acid on liver fibrogenesis. Figure 3 shows typical Azan staining results, in which fibrous materials are stained blue. In the controls (Fig. 3A), hardly any blue staining was observed in the pericentral area. In contrast, the livers injured by chronic CCl_4 treatment displayed a considerable accumulation of fibrous materials (Fig. 3B). CCl_4 treatment for 4 weeks caused an excessive deposition of collagen fibrils that was sufficient for the evaluation of the antifibrogenic effect of syringic acid and vanillic acid. Based on the results of Azan staining, the syringic acid and vanillic acid treatments obviously suppressed collagen accumulation (Figs. 3D, E). To quantitatively evaluate the effect of syringic acid and vanillic acid on fibrogenesis, we

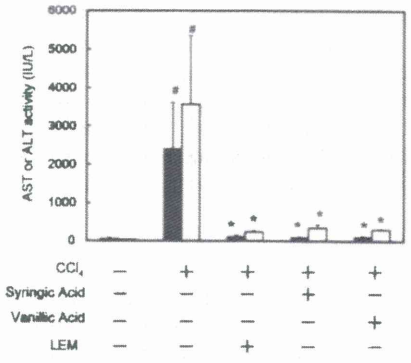

Fig. 2. Effect of Syringic Acid and Vanillic Acid on CCl_4-Induced Chronic Hepatic Injury

Mice received an intraperitoneal injection of CCl_4 and an intravenous injection of L.E.M., syringic acid, or vanillic acid twice a week for 4 weeks. The serum levels of AST (solid column) and ALT (open column) were determined. The values are mean±S.D ($n=4$). The data were analyzed by Student's t-test ($\#p<0.05$, as compared to uninjured control mice) and Dunnett's method ($*p<0.05$, as compared to CCl_4-injured control mice).

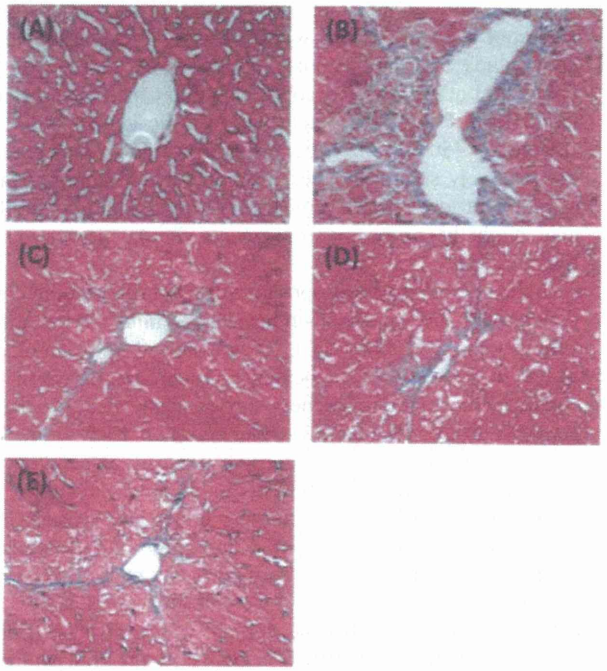

Fig. 3. Azan Staining of Liver Sections

Livers were excised from normal mice (A), CCl_4-injured control mice (B), L.E.M.-treated mice (C), syringic acid-treated mice (D), and vanillic acid-treated mice (E). Original magnification ×400.

measured the hepatic hydroxyproline content, which parallels the extent of fibrosis. After 4 weeks of CCl_4 treatment, the hepatic hydroxyproline content increased 4.6-fold as compared with the controls (Fig. 4). The intravenous administration of syringic acid or vanillic acid significantly decreased the hepatic hydroxyproline content. These data suggest that syringic acid and vanillic acid can suppress hepatic fibrosis in chronic liver injury. Next, we measured the amount of malondialdehyde in the liver samples as a marker of oxidative stress. The malondialdehyde content was drastically increased after 4 weeks of CCl_4 treatment, but the intravenous administration of syringic acid or vanillic acid significantly

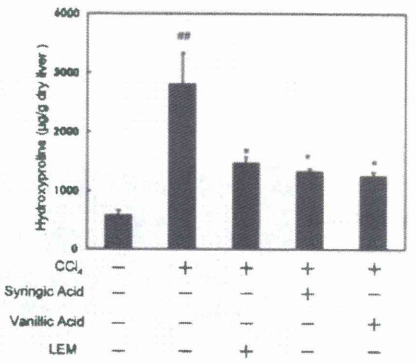

Fig. 4. Effect of Syringic Acid and Vanillic Acid on the Hydroxyproline Content of the Liver

The hydroxyproline content of the liver was measured after 4 weeks of treatments. The values are mean±S.D. ($n=4$). The data were analyzed by Student's t-test ($\#\#p<0.01$, as compared to uninjured control mice) and Dunnett's method ($*p<0.05$, as compared to CCl_4-injured control mice).

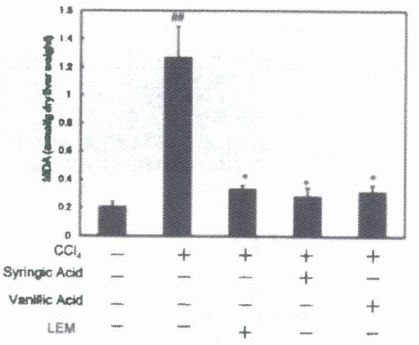

Fig. 5. Effect of Syringic Acid and Vanillic Acid on the Suppression of Oxidative Stress

The malondialdehyde content of the liver was determined after 4 weeks of experiments. The values are mean±S.D. ($n=4$). The data were analyzed by Student's t-test ($\#\#p<0.01$, as compared to uninjured control mice) and Dunnett's method ($*p<0.05$, as compared to CCl_4-injured control mice).

decreased the malondialdehyde content to an almost normal level (Fig. 5). The protective effects of syringic acid and vanillic acid were almost comparable to that of L.E.M. (Figs. 2—5).

***In Vitro* Effect on HSC Activation and Hepatocyte Viability** We examined the direct effect of syringic acid and vanillic acid on the activation of HSCs, which play a central role in liver fibrogenesis, using the monolayer culture. HSCs are activated during the monolayer culture to transform into proliferating myofibroblast-like cells. As shown in Fig. 6A, HSCs were activated after 7 d of culture to be fibroblastic cell-type. The addition of syringic acid or vanillic acid dose-dependently suppressed the activation (Fig. 6B). HSCs maintained their quiescent state by the addition of more than 0.5 mg/ml of the respective compound. Next, the effect of syringic acid and vanillic acid on gene expression of Type I collagen and α-SMA, which are markers of activated HSCs, was examined. HSCs were cultured for 7 d in the presence or absence of syringic acid or vanillic acid, and the gene expression was analysed by RT-PCR. As shown in Fig. 7, syringic acid and vanillic acid remarkably suppressed the expression of collagen and α-SMA genes, indicating that the phenolic compounds directly act on HSCs and suppress the activation

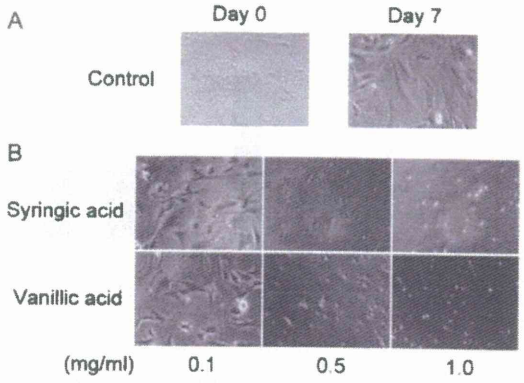

Fig. 6. Phase-Contrast Micrographs of Cultured HSCs

Freshly isolated HSCs were cultured for 7 d in the absence (A) and presence (B) of syringic acid or vanillic acid at the indicated concentration. Original magnification ×200.

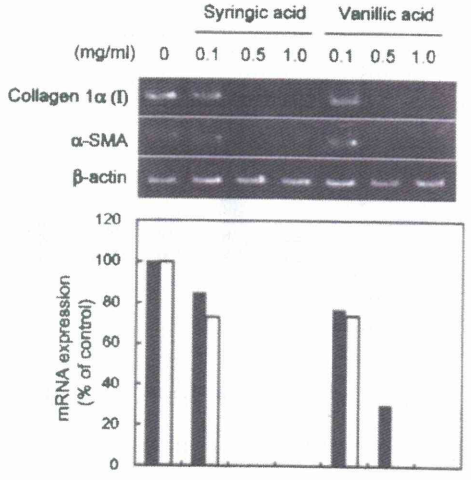

Fig. 7. RT-PCR Analysis of Gene Expression Relating to HSC Activation

Bottom figure shows the relative expression of collagen I α(I) (closed bar) and α-SMA (open bar) compared with the non-addition control.

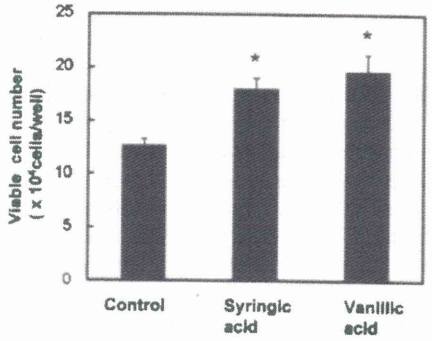

Fig. 8. Effect of Syringic Acid and Vanillic Acid on Viability of Cultured Hepatocytes

Freshly isolated hepatocytes were cultured for 24 h in the absence or presence of 1.0 mg/ml syringic acid or vanillic acid. Viability was measured by trypan blue exclusion test. The data were analyzed by Dunnett's method (* $p<0.05$, as compared to control).

to maintain the quiescent state. We then examined the effect of the compounds on liver parenchymal hepatocytes using the primary culture (Fig. 8). Hepatocytes were isolated and cultured in the presence or absence of syringic acid or vanillic acid. After 24 h of culture, viable cells were counted using trypan blue exclusion test. The addition of syringic acid or vanillic acid significantly maintained viability of cultured hepatocytes. These results suggested that syringic acid or vanillic acid might suppress liver fibrogenesis and inflammation by inhibiting HSC activation and protecting hepatocytes, respectively in chronically liver injured mice.

DISCUSSION

The physiological functions of plant-derived phenolic compounds have been extensively reported.[7,13,14] Syringic acid and vanillic acid possess antimicrobial, anti-cancer, and anti-DNA oxidation properties.[15—17] We recently found that syringic acid and vanillic acid could act as immunomodulators in mice with ConA-induced liver injury.[8] In the present study, we show that syringic acid and vanillic acid have protective effects in mice with CCl_4-induced liver injury. Both phenolic compounds dramatically suppressed liver fibrogenesis in the chronic CCl_4-treatment model. When these phenolics are orally administered to hamsters, they are adsorbed and appear in the blood within 40 min.[18] Although these compounds are intravenously administered in the present study, oral administration could also elicit the hepatoprotective effect. The syringic acid and vanillic acid contents in L.E.M. are 450 and 378 μg/g, respectively. Thus, the contents are relatively small, but these compounds are commercially available at low prices. Therefore, syringic acid and vanillic acid might be promising oral agents for the prevention of liver disease.

We evaluated the hepatoprotective effect of phenolic compounds in mice with CCl_4-induced liver injury. After intravenous administration, CCl_4 is introduced into the liver, where it is toxic to hepatocytes. Cytochrome P-450 in the endoplasmic reticulum of hepatocytes catalyzes the dehalogenation to produce an unstable complex trichloromethyl radical,[19] resulting in the extensive necrosis of hepatocytes that leads to liver inflammation. In the present study, the transaminase level in the serum was drastically increased by CCl_4 treatment. Generation of ROS degrade polyunsaturated lipids to form malondialdehyde, which is a marker of oxidative stress. The chronic CCl_4 treatment significantly increased the malondialdehyde content of the liver. Syringic acid and vanillic acid clearly suppressed the transaminase and malondialdehyde levels in CCl_4-treated mice. Since both of these compounds have 1,1-diphenyl-2-picrylhydrazyl (DPPH) radical scavenging activity,[8] the suppression of ROS generation appears to be responsible for the hepatoprotective effect. Moreover, the CCl_4-induced liver fibrogenesis was suppressed by the administration of syringic acid and vanillic acid. The activation of HSCs is responsible for the development of liver fibrosis.[20,21] During liver injury with persistent inflammation, HSCs are activated to differentiate into proliferating myofibroblast-like cells and overproduce extracellular matrix, leading to fibrogenesis. Since HSCs are activated spontaneously during cell culture,[22] we examined the effect of syringic acid and vanillic acid on the activation of primary cell cultures of rat HSCs. Both of these compounds clearly inhibited the change from spherical to spindle shape and the expression of α-smooth muscle actin and collagen Type Iα genes, which are the markers of HSC activation. We also

examined the effect of syringic acid and vanillic acid on the maintenance of hepatocyte viability *in vitro*. Both of these compounds significantly maintained the viability of primary cell cultures of hepatocytes. Thus, syringic acid and vanillic acid could directly exert a physiological effect on hepatocytes and HSCs. Both phenolic compounds might affect CCl_4 metabolism to inhibit the generation of cytotoxic trichloromethyl radical in the liver. However, the direct effects of syringic acid and vanillic acid on HSCs and hepatocytes were shown in this study, and the protective effect was also shown in ConA-induced liver injured mice in our previous study.[8] Moreover, these phenolic compounds have strong radical scavenging activity. These results suggest that during the repeated treatment of CCl_4, these compounds could protect hepatocytes and HSCs from CCl_4-induced oxidative stress to suppress liver inflammation and fibrogenesis.

The hot-water extracts from cultured mycelia of *L. edodes* have versatile physiological effects and might contain promising seed compounds for pharmaceutical development. We have shown that syringic acid and vanillic acid have anti-oxidative and immunomodulating activities. In addition to these phenolics, L.E.M. could contain novel compounds with pharmaceutical potential. We are currently trying to isolate bioactive components from L.E.M.

REFERENCES

1) Wasser S. P., Weis A. L., *Crit. Rev. Immunol.*, **19**, 65—96 (1999).
2) Suzuki H., Okubo A., Yamazaki S., Suzuki K., Mitsuya H., Toda S., *Biochem. Biophys. Res. Commun.*, **160**, 367—373 (1989).
3) Yamamoto Y., Shirono H., Kono K., Ohashi Y., *Biosci. Biotechnol. Biochem.*, **61**, 1909—1912 (1997).
4) Yamada T., Oinuma T., Niihashi M., Mitsumata M., Fujioka T., Hasegawa K., Nagaoka H., Itakura H., *J. Atheroscler. Thromb.*, **9**, 149—156 (2002).
5) Aggarwal B. B., Kumar A., Bharti A. C., *Anticancer Res.*, **23**, 363—398 (2003).
6) Aviram M., Dornfeld L., Kaplan M., Coleman R., Gaitini D., Nitecki S., Hofman A., Rosenblat M., Volkova N., Presser D., Attias J., Hayek T., Fuhrman B., *Drugs Exp. Clin. Res.*, **28**, 49—62 (2002).
7) Levites Y., Weinreb O., Maor G., Youdim M. B., Mandel S., *J. Neurochem.*, **78**, 1073—1082 (2001).
8) Itoh A., Isoda K., Kondoh M., Kawase M., Kobayashi M., Tamesada M., Yagi K., *Biol. Pharm. Bull.*, **32**, 1215—1219 (2009).
9) Forrester I. T., Grabski A. C., Mishra C., Kelley B. D., Strickland W. N., Leatham G. F., Burgess R. R., *Appl. Microbiol. Biotechnol.*, **33**, 359—365 (1990).
10) Kivirikko K. I., Laitinen O., Prockop D. J., *Anal. Biochem.*, **19**, 249—255 (1967).
11) Kawada N., Tran-Thi T. A., Klein H., Decker K., *Eur. J. Biochem.*, **213**, 815—823 (1993).
12) Seglen P. O., *Methods Cell Biol.*, **13**, 29—83 (1976).
13) Gao X., Xu Y. X., Janakiraman N., Chapman R. A., Gautam S. C., *Biochem. Pharmacol.*, **62**, 1299—1308 (2001).
14) Aggarwal S., Ichikawa H., Takada Y., Sandur S. K., Shishodia S., Aggarwal B. B., *Mol. Pharmacol.*, **69**, 195—206 (2006).
15) Aziz N. H., Farag S. E., Mousa L. A., Abo Zaid M. A., *Microbios*, **93**, 43—54 (1998).
16) Guimaraes C. M., Giao M. S., Martinez S. S., Pintado A. I., Pintado M. E., Bento L. S., Malcata F. X., *J. Food Sci.*, **72**, C039–C043 (2007).
17) Kampa M., Alexaki V. I., Notas G., Nifli A. P., Nistikaki A., Hatzoglou A., Bakogeorgou E., Kouimtzoglou E., Blekas G., Boskou D., Gravanis A., Castanas E., *Breast Cancer Res.*, **6**, R63–R74 (2004).
18) Chen C. Y., Milbury P. E., Kwak H. K., Collins F. W., Samuel P., Blumberg J. B., *J. Nutr.*, **134**, 1459—1466 (2004).
19) Castillo T., Koop D. R., Kamimura S., Triadafilopoulos G., Tsukamoto H., *Hepatology*, **16**, 992—996 (1992).
20) Albanis E., Friedman S. L., *Clin. Liver Dis.*, **10**, 821—833 (2006).
21) Friedman S. L., *Toxicology*, **254**, 120—129 (2008).
22) Sato M., Suzuki S., Senoo H., *Cell Struct. Funct.*, **28**, 105—112 (2003).

Biomaterials 31 (2010) 5463–5471

Contents lists available at ScienceDirect

Biomaterials

journal homepage: www.elsevier.com/locate/biomaterials

Mucosal vaccination using claudin-4-targeting

Hideki Kakutani [a], Masuo Kondoh [a,*], Masahiro Fukasaka [a], Hidehiko Suzuki [a], Takao Hamakubo [b], Kiyohito Yagi [a,**]

[a] Laboratory of Bio-Functional Molecular Chemistry, Graduate School of Pharmaceutical Sciences, Osaka University, Suita, Osaka 565-0871, Japan
[b] Department of Molecular Biology and Medicine, Research Center for Advanced Science and Technology, The University of Tokyo, Meguro, Tokyo 153-8904, Japan

ARTICLE INFO

Article history:
Received 12 January 2010
Accepted 19 March 2010
Available online 17 April 2010

Keywords:
Immunomodulation
Mucosa
Drug delivery
Epithelium

ABSTRACT

Mucosa-associated lymphoid tissue (MALT) plays pivotal roles in mucosal immune responses. Efficient delivery of antigens to MALT is a critical issue for the development of mucosal vaccines. Although claudin-4 is preferentially expressed in MALT in the gut, a claudin-4-targeting approach for mucosal vaccination has never been developed. In the present study, we found that claudin-4 is expressed in nasal MALT, and we prepared a fusion protein of ovalbumin (OVA) as a model antigen with a claudin-4-binder, the C-terminal fragment of *Clostridium perfringens* enterotoxin (C-CPE) (OVA-C-CPE). Nasal immunization with OVA-C-CPE, but not a mixture of OVA and C-CPE, induced the production of OVA-specific serum IgG and nasal, vaginal and fecal IgA. Deletion of the claudin-4-binding region in OVA-C-CPE attenuated the induction of the immune responses. OVA-C-CPE immunization activated both Th1 and Th2 responses, and nasal immunization with OVA-C-CPE showed anti-tumor activity in mice inoculated with OVA-expressing thymoma cells. These results indicate that the claudin-4-targeting may be a potent strategy for nasal vaccination.

1. Introduction

Each year, 17 million people die from infectious diseases worldwide, and 7 million people die from cancers worldwide (http://www.globalhealth.org/infectious_diseases/; http://www.reuters.com/article/healthNews/idUSN16330649200712 17). Thus, the development of methods to prevent and treat infectious diseases and cancers is an important issue for healthcare worldwide. Vaccination against these diseases is a promising approach because of its low frequency of side effects and its great preventative and therapeutic effects. Vaccination strategies are classified as parenteral or mucosal. Parenteral vaccination is effective for the elimination of infectious cells and cancer cells by the induction of systemic immune responses. Parenteral vaccines are administered by injections, which are invasive, painful, and have low levels of patient compliance; moreover, mucosal immunological defense is not induced. In contrast, mucosal vaccine elicits both mucosal and systemic immune responses, resulting in the prevention of infection on the mucosal surfaces and the elimination of pathological cells [1–3]. Mucosal administration is needle-free, less painful, and has improved patience compliance. Thus, mucosal vaccination appears to be an ideal vaccination strategy, although mucosally administered protein antigens are poorly immunogenic. Various approaches for the mucosal delivery of antigens have been investigated [4–6]. Mucosa-associated lymphoid tissues (MALTs) play pivotal roles in mucosal immunological responses [7,8]. MALTs comprise gut-associated lymphoid tissues (GALT), nasopharynx-associated lymphoid tissue (NALT) and bronchus-associated lymphoid tissue (BALT). MALT contains lymphocytes, M cells, T cells, B cells and antigen-presenting cells (APCs), and the efficient delivery of antigens into MALT is essential for mucosal vaccinations [9]. Indeed, there have been several attempts to deliver antigens to MALT using microparticles, liposomes, saponins or chitosans [4–6].

Immunization at one mucosal surface can generate secretory IgA responses at other mucosal sites. Ideally, vaccination at a single site would provide both humoral and cell-mediated protection, not only

Abbreviations: MALT, mucosa-associated lymphoid tissue; OVA, ovalbumin; C-CPE, C-terminal fragment of *Clostridium perfringens* enterotoxin; OVA-C-CPE, fusion proteins of OVA and C-CPE; GALT, gut-associated lymphoid tissue; NALT, nasopharynx-associated lymphoid tissue; BALT, bronchus-associated lymphoid tissue; APC, antigen-presenting cell; FAE, follicle-associated epithelium; TJ, tight junction; CPE, *Clostridium perfringens* enterotoxin; RT-PCR, reverse transcriptase-polymerase chain reaction; SDS-PAGE, sodium dodecyl sulfate-polyacrylamide gel electrophoresis; PBS, phosphate-buffered saline; ELISA, enzyme-linked immunosorbent assay; BV, budded baculovirus; FBS, fetal bovine serum; TBS, tris-buffered saline; IFN, interferon; IL, interleukin.

* Corresponding author. Tel.: +81 6 6879 8196; fax: +81 6 6879 8199.
** Corresponding author. Tel./fax: +81 6 6879 8195.
E-mail addresses: masuo@phs.osaka-u.ac.jp (M. Kondoh), yagi@phs.osaka-u.ac.jp (K. Yagi).

0142-9612/$ – see front matter © 2010 Elsevier Ltd. All rights reserved.
doi:10.1016/j.biomaterials.2010.03.047

at the relevant mucosal surface, but also throughout the body [4]. In this regard, nasal vaccination has shown particular potential. Nasally administered vaccines induced mucosal IgA antibody responses in the salivary glands, respiratory tracts, genital tracts, and intestines [10–12]. The nasal route can also induce cytotoxic T lymphocytes in distant mucosal tissues including the female genital tract [13]. Additionally, nasal immunization produced greater systemic antibody responses than other mucosal immunization routes [12,14]. However, despite these encouraging characteristics, free antigens are usually unable to stimulate immune responses following intranasal administration due to their ineffective delivery to immune response-inducing sites [15]. Thus, the effective delivery of antigens to NALT is needed for the development of a potent nasal vaccine.

A single layer of epithelial cell sheet follicle-associated epithelium (FAE) covers NALT. FAE contains M cells, which are key antigen-sampling cells for the delivery of mucosally encountered antigens to the underlying APCs, and FAE plays a pivotal role in the mucosal immunological response [16–18]. Antigen delivery using a ligand for the FAE that covers NALT would be a potent strategy for the development of a mucosal vaccine. Epithelium has well-developed tight junctions (TJs) that seal the intercellular space on the epithelial cell sheets [19,20]. Occludin, claudin and junctional adhesion molecule are components of TJs [21]. Among these components, claudin-4 was preferentially expressed on the dome region of FAE in GALT [22]. We found that claudin-4 was also expressed in NALT (Fig. 1). These findings strongly indicate that claudin-4-targeting may be useful for mucosal vaccines; however, a mucosal vaccine that uses a claudin-4-binder has never been developed.

Clostridium perfringens enterotoxin (CPE) causes food poisoning in humans [23]. A receptor for CPE is claudin-4, and the C-terminal fragment of CPE (C-CPE) is a claudin-4-binder [24–26]. We previously prepared a claudin-4-targeting cytotoxic molecule by genetically fusing a cytotoxin with C-CPE [27,28]. In the present study, we investigated whether claudin-4-targeting is a potent strategy for mucosal vaccine using C-CPE-fused antigen protein.

2. Materials and methods

2.1. Animals

Female BALB/c mice and C57BL/6 mice (6–8 weeks old) were purchased from SLC, Inc. (Shizuoka, Japan). The mice were housed at 23 ± 1.5 °C with a 12-h light/dark cycle and were allowed free access to standard rodent chow and water. After their arrival, the mice were allowed to adapt to their environment for at least 1 week before the experiments. The animal experiments were performed according to the guidelines of Osaka University.

2.2. Reverse transcriptase-polymerase chain reaction (RT-PCR)

Total mRNA was extracted from NALT using Isogen (Nippongene, Toyama, Japan), and the mRNA was reverse-transcribed using an RNA PCR kit (AMV, Ver.3.0) according to the manufacturer's instructions (Takara, Kyoto, Japan). The polymerase chain reaction (PCR) amplification from the resultant cDNA was performed using primer pairs for claudin-4 (forward, 5′-tggatgaactgcgtggtg-3′; reverse, 5′-ggttgtagaagtcgcggatg-3′) for 35 reaction cycles (94 °C, 45 s; 52 °C, 60 s; 72 °C, 30 s) or β-actin (forward, 5′-tagatgggcacagtgtggg-3′; reverse, 5′-ggcgtgatggtgggcatgg-3′) for 30 reaction cycles (94 °C, 30 s; 58 °C, 60 s; 72 °C, 30 s). The amplified products were separated by electrophoresis on a 2% agarose gel and visualized with ethidium bromide.

2.3. Immunoblotting for claudin-4

NALT was lysed in a lysis buffer (50 mM Tris–HCl, pH 7.5, 0.15 M NaCl, 0.1% Triton X-100, 0.1% SDS, 1 mM sodium orthovanadate, 1 mM EDTA, 1 mM NaF, and 1 mM phenylmethylsulfonyl fluoride). The lysates (10 μg of protein) were subjected to sodium dodecyl sulfate-polyacrylamide gel electrophoresis (SDS-PAGE) followed by western blotting with anti-claudin-4 (Zymed Laboratory, South San Francisco, CA) or anti-β-actin antibodies (Sigma–Aldrich, St. Louis, MO). The immunoreactive bands were detected with a peroxidase-labeled secondary antibody followed by visualization with a chemiluminescence reagent (Amersham Bioscience, Piscataway, NJ).

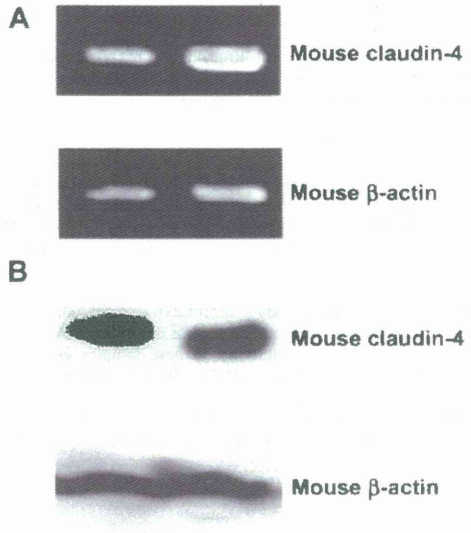

Fig. 1. Expression of claudin-4 in NALT. A) RT-PCR analysis. mRNA was isolated from NALT of mice, and expression of claudin-4 was assayed by RT-PCR. B) Immunoblot analysis. The lysate of NALT was subjected to SDS-PAGE, followed by western blotting with anti-claudin-4 Ab. β-actin was used as an internal control.

2.4. Preparation of OVA-C-CPE fusion proteins

We prepared expression plasmids encoding fusion proteins of OVA with C-CPE or C-CPE303, in which the claudin-4-binding C-terminal 16 amino acids of C-CPE were deleted [29]. Oligonucleotides containing a G4S linker and multiple cloning sites, including KpnI, SpeI, SmaI and PacI sites, were subcloned into NdeI-digested pET16b (Novagen, Darmstadt, Germany), pET-C-CPE and pET-C-CPE303 [30], resulting in pET-MCS and pET-MCS-C-CPEs. OVA cDNA was PCR amplified using pCMV Script/OVA (Kindly provided from Dr. S. Nakagawa, Osaka University, Japan) as a template, a forward primer (5′-gcggtaccatgggctccatcggcgcagc-3′, KpnI site is underlined), and a reverse primer (5′-ccttaattaaaggggaaacacatctgccaa-3′, PacI site is underlined). The resulting OVA fragment was inserted into pET-MCS and pET-MCS-C-CPEs at the KpnI/PacI site, resulting in pET-OVA, pET-OVA-C-CPE and pET-OVA-C-CPE303. The OVA-fusion protein plasmids were transduced into *Escherichia coli* strain BL21 (DE3), and the production of OVA and OVA-C-CPEs was induced by the addition of isopropyl-D-thiogalactopyranoside. The harvested cells were lysed in buffer A (10 mM Tris–HCl, pH 8.0, 400 mM NaCl, 5 mM $MgCl_2$, 0.1 mM PMSF, 1 mM 2-mercaptoethanol, and 10% glycerol) supplemented with 8 M urea when necessary. The lysates were applied to HiTrap™ HP (GE Healthcare, Buckinghamshire, UK), and the fusion proteins were eluted with buffer A containing 100–500 mM imidazole. The solvent was exchanged with phosphate-buffered saline (PBS) using a PD-10 column (GE Healthcare), and the purified protein was stored at −80 °C until use. Purification of the fusion proteins was confirmed by SDS-PAGE, followed by staining with Coomassie Brilliant Blue and by immunoblotting with anti-his-tag antibody. Protein assays were performed using a BCA protein assay kit (Pierce Chemical, Rockford, IL) with bovine serum albumin as a standard.

2.5. Enzyme-linked immunosorbent assay (ELISA)

Budded baculovirus (BV) displaying mouse claudin-1 or -4 was prepared as described previously [28]. Briefly, the DNA fragments of claudin-1 or -4 were subcloned into the baculoviral transfer vector pFastBac1 (Invitrogen, Gaithersburg, MD). Recombinant baculoviruses were generated using the Bac-to-Bac system (Invitrogen). Sf9 cells maintained in Grace's Insect medium containing 10% fetal bovine serum (FBS) at 27 °C were infected with the recombinant baculoviruses. After 70 h, the conditioned medium was recovered and centrifuged. The resultant pellets of the BV fraction were suspended in Tris-buffered saline (TBS) containing protease inhibitor cocktail and then stored at 4 °C until use.

The BV displaying claudins was diluted with TBS and adsorbed to the wells of 96-well ELISA plates (Greiner Bio-One, Tokyo, Japan) overnight at 4 °C. The wells were blocked with TBS containing 1.6% BlockAce (Dainippon Sumitomo Pharmaceutical, Osaka, Japan) for 2 h at room temperature and the C-CPE, OVA-C-CPE or OVA-C-CPE303 was added. After 2-h incubation, the wells were washed and incubated with anti-his-tag antibody followed by a horseradish peroxidase-conjugated secondary antibody. The immunoreactive proteins were detected using TMB peroxidase substrate at an absorbance of 450 nm.

2.6. Nasal immunization

Mice were nasally immunized with 10-μl aliquots of OVA, a mixture of OVA and C-CPE, OVA-C-CPE or OVA-C-CPE303 at the indicated schedules. The doses of the proteins were equal to 5 μg of OVA and 1.89 μg of C-CPE.

2.7. OVA-specific antibody production

Seven days after the last immunization, serum and mucosal secretions (nasal washes, vaginal washes, and fecal extracts) were collected. Fecal pellets (100 mg) were suspended in 1 ml of PBS and extracted by vortexing for 10 min. The samples were centrifuged at 3000×g for 10 min, and the resultant supernatants were used as fecal extracts. Vaginal and nasal mucosa were washed with 100 or 200 μl of PBS, respectively.

The titers of OVA-specific antibody in serum, extracts and mucosal washes were determined by ELISA. Briefly, an immunoplate was coated with OVA (100 μg/well in a 96-well plate). Ten-fold serial dilutions of these samples were added to the immunoplate followed by the addition of horseradish peroxidase-conjugated anti-mouse IgG, IgG1, IgG2a or IgA. The OVA-specific antibodies were detected using TMB peroxide substrate. End-point titers were expressed as the dilution ratio, which gave 0.1 above control values obtained for serum of naïve mice at an absorbance of 450 nm.

2.8. Cytokine ELISA

Serum interferon γ (IFN-γ) and Interleukin-13 (IL-13) were measured with an ELISA kit according to the manufacturer's protocol (R&D Systems, Inc., MN).

2.9. Cell cultures

A murine thymoma cell line EL4 (H-2^b) was cultured in RPMI 1640 supplemented with 10% FBS. EG7-OVA cells (OVA-transfected EL4 cells) were maintained in RPMI 1640 containing 10% FBS in the presence of 400 μg/ml of G418.

2.10. Anti-tumor activity

In an anti-tumor assay, female C57BL/6 mice (6–8 weeks) were nasally immunized with vehicle, OVA, a mixture of OVA and C-CPE, OVA-C-CPE or OVA-C-CPE303 once a week for 3 weeks. All non-vehicle immunizations contained equivalent amounts of OVA (5 μg). Seven days after the last immunization, the mice were subcutaneously inoculated with 1×10^6 EG7-OVA cells. Tumor growth was monitored by measuring two diameters, and the tumor volume was calculated as $a \times b \times b/2$, where a is the maximum diameter of the tumor and b is the minimum diameter of the tumor.

2.11. Statistical analysis

Results were analyzed by an analysis of variance (ANOVA) followed by the Dunnett multiple comparison test, and statistical significance was assigned at $p < 0.05$.

3. Results

3.1. Expression of claudin-4 in NALT

Nasal vaccine is a potent therapy for infectious diseases and cancers since nasal vaccination potentiates humoral and cellular immune responses throughout the body. NALT is the nasal lymphoid tissue, and effective delivery of antigens to NALT is critical for the development of mucosal vaccinations. A previous report showed that claudin-4 is expressed in GALT [22], whereas it is unclear whether claudin-4 is expressed in NALT. To investigate the expression of claudin-4 in NALT, NALT was isolated from mice, and the NALT lysate was subjected to RT-PCR and immunoblotting analyses. As shown in Fig. 1A and B, claudin-4 mRNA and protein were detected in NALT. These data indicate that claudin-4-binder may be a targeting molecule for NALT.

3.2. Preparation of claudin-4-targeting OVA

Claudin has low antigenicity, and there has been little success in the preparation of antibodies against the extracellular region of claudin. C-CPE corresponding to aa 184–319 at the C-terminal of CPE is a claudin-4-binder [24,25]. We previously prepared a claudin-4-targeting cytotoxic molecule genetically fused with C-CPE [27]. To evaluate whether a claudin-4-targeting strategy is an effective method for mucosal vaccination, we genetically fused C-CPE with OVA, a popular model antigen for vaccination, to yield OVA-C-CPE (Fig. 2A). OVA-C-CPE was produced by *E. coli* and purified by affinity chromatography. Purification of the protein was confirmed by SDS-PAGE and immunoblotting (Fig. 2B). The molecular size was identical to the predicted size of 62 kDa for OVA-C-CPE. To evaluate the binding of OVA-C-CPE to claudin-4, we performed ELISA with a claudin-displaying BV-coated immunoplate. OVA-C-CPE or C-CPE was added to wells coated with wild-type BV, claudin-1-BV or claudin-4-BV. The bound proteins were detected using anti-his-tag antibody. Like C-CPE, OVA-C-CPE bound to claudin-4-BV but not wild-type BV or claudin-1-BV (Fig. 2C).

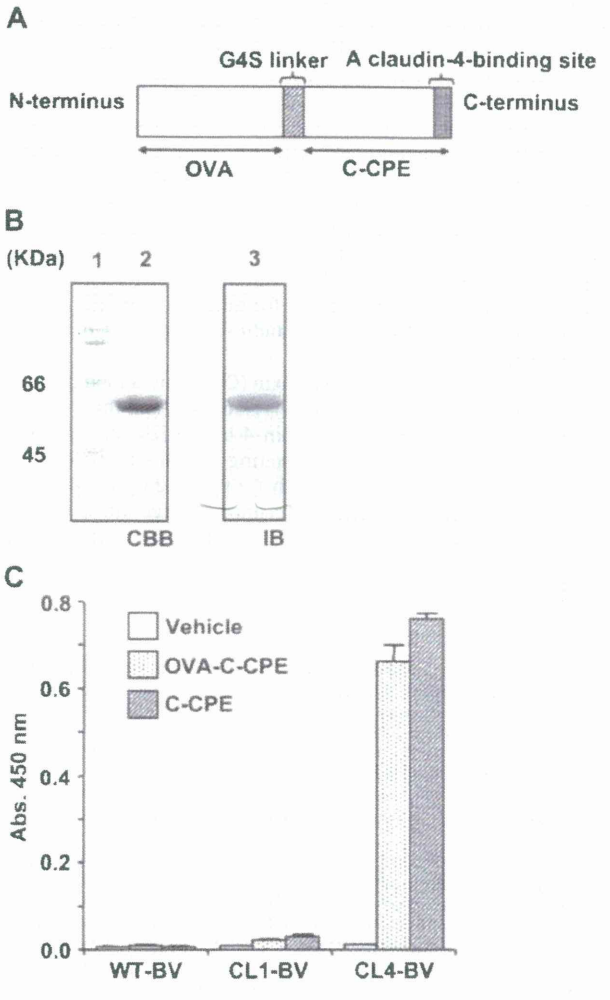

Fig. 2. Preparation of OVA-C-CPE. A) Schematic illustration of OVA-C-CPE. The claudin-4-binding site of C-CPE is located in the C-terminal 16 amino acids [29]. OVA was fused with C-CPE at the N-terminal of C-CPE, resulting in OVA-C-CPE. B) Purification of OVA-C-CPE. OVA-C-CPE was expressed in *E. Coli* as a his-tagged protein and isolated by Ni-affinity chromatography. The purification of OVA-C-CPE was confirmed by SDS-PAGE followed by staining with Coomassie Brilliant Blue (CBB, left panel) and by immunoblotting with an anti-his-tag antibody (IB, right panel). Lane 1: molecular weight marker; lane 2, 3: OVA-C-CPE. The putative molecular mass of OVA-C-CPE is 62 kDa. C) Binding of OVA-C-CPE to claudin-4. Wild-type BV (WT-BV), BV displaying claudin-1 (CL1-BV) or -4 (CL4-BV) was absorbed onto a 96-well immunoplate, and then vehicle, OVA-C-CPE or C-CPE was added to the well. OVA-C-CPE or C-CPE bound to BV was detected by an anti-his-tag Ab followed by horseradish peroxidase-labeled secondary Ab. C-CPE was used as a positive control for a claudin-4-binding. Data are means ± SD ($n = 4$).

3.3. Induction of OVA-specific humoral responses

To clarify whether claudin-4-targeting activates an immune response, we investigated antigen-specific humoral responses at both systemic and mucosal sites in mice that received nasally administered OVA-C-CPE. Mice received an intranasal administration of OVA, a mixture of OVA and C-CPE, or OVA-C-CPE fusion protein once a week for 3 weeks. Seven days after the last administration, we measured the OVA-specific serum IgG, nasal IgA, vaginal IgA and fecal IgA levels. As shown in Fig. 3A, the OVA-specific serum IgG responses were increased in mice immunized with OVA-C-CPE as compared to the mice immunized with OVA or a mixture of OVA and C-CPE. The OVA-specific IgA responses in nasal washes were greater from mice immunized with OVA-C-CPE than from mice immunized with OVA or a mixture of OVA and C-CPE (Fig. 3B). It is a superior character of mucosal vaccination that antigen-specific IgA responses were induced not only at the immunized site but also at remote mucosal surfaces [4]. As shown in Fig. 3C and D, nasal immunization with OVA-C-CPE activated vaginal and fecal OVA-specific IgA responses. The OVA-specific IgA responses did not occur in mice immunized with a mixture of OVA and C-CPE. These data suggest that fusion of OVA with C-CPE is critical for successful nasal vaccination.

We previously found that the C-terminal 16 amino acids of C-CPE are essential for claudin-4-binding [29]. To investigate the involvement of claudin-4 in OVA-specific humoral responses in mice nasally immunized with OVA-C-CPE, we prepared OVA-C-CPE303, in which the claudin-4-binding region was deleted (Fig. 4A). Deletion of the 16 amino acid region attenuated the claudin-4-binding of OVA-C-CPE (Fig. 4B). OVA-specific serum IgG and nasal, vaginal and fecal mucosal IgA responses were also attenuated in mice immunized with OVA-C-CPE303 (Fig. 4C and D, 4E and F, respectively). No histological mucosal injury was found after nasal immunization with OVA-C-CPE (data not shown). These findings indicate that claudin-4-targeting may be involved in nasal vaccination by OVA-C-CPE.

3.4. Induction of Th1 and Th2 responses by OVA-C-CPE

Nasal immunization of antigen induced antigen-specific immune responses including Th1- and Th2-type responses [31,32]. We next investigated whether nasal immunization with OVA-C-CPE evoked Th1- or Th2-type responses. The OVA-specific IgG1 (a Th2 response) and IgG2a (a Th1 response) responses in the serum of mice nasally immunized with OVA-C-CPE were significantly enhanced compared to those of mice immunized with OVA alone or a mixture of OVA and C-CPE (Fig. 5A). Measurement of Th1 (IFN-γ) and Th2 (IL-13)-specific cytokines in splenocytes isolated from mice nasally immunized with OVA, a mixture of OVA and C-CPE, or OVA-C-CPE showed that nasal immunization with OVA-C-CPE increased both Th1 and Th2 cytokine production (Fig. 5B). Th1 and

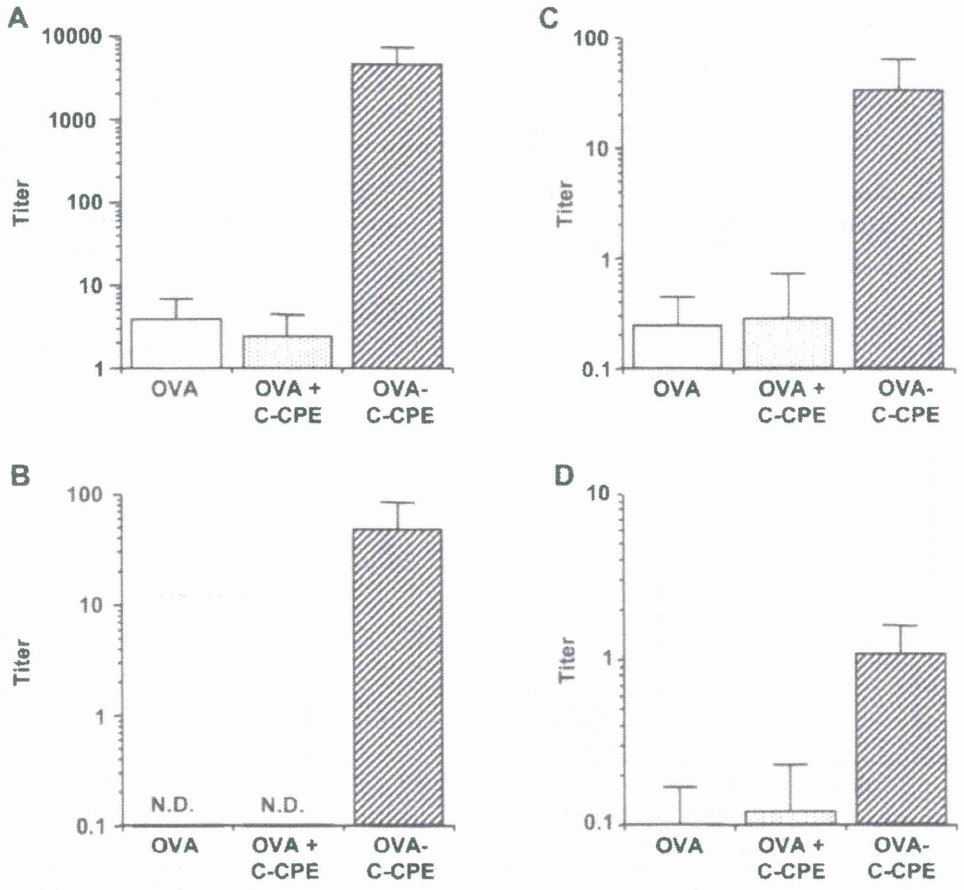

Fig. 3. Production of OVA-specific IgG and IgA by OVA-C-CPE. Mice were nasally immunized with vehicle, OVA, a mixture of OVA and C-CPE, or OVA-C-CPE (5 μg OVA) once a week for 3 weeks. Seven days after the last immunization, the levels of serum IgG (A), nasal IgA (B), vaginal IgA (C) and fecal IgA (D) were determined by ELISA. Data are means ± SD ($n = 4$). The results are representative of three independent experiments. N.D., not detected.

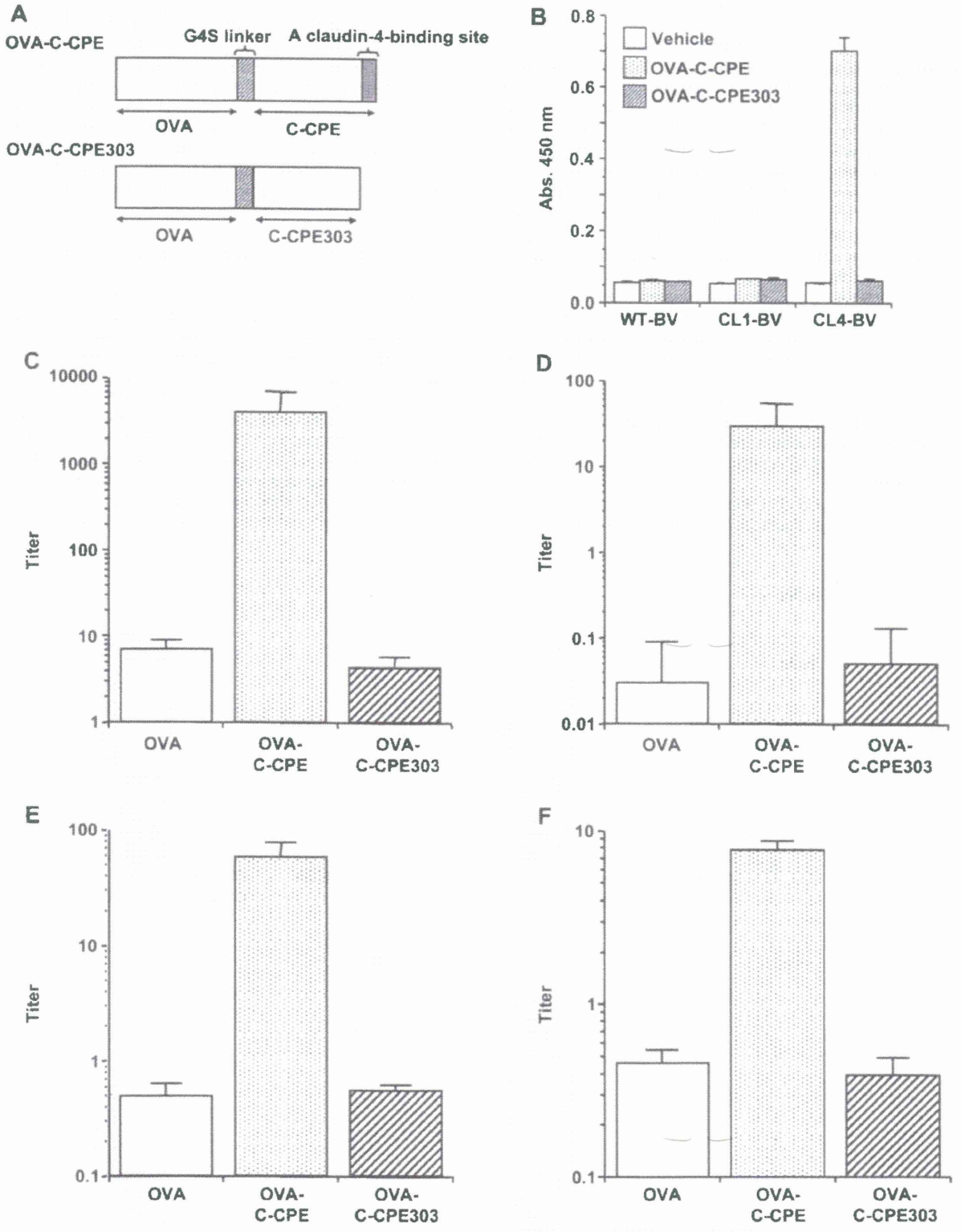

Fig. 4. Involvement of claudin-4 in the immune responses to OVA-C-CPE. A) Schematic illustration of OVA-C-CPE mutant. The C-terminal 16 amino acid-deleted C-CPE mutant (C-CPE303) did not bind to claudin-4 [29]. To clarify the involvement of claudin-4 in the immune response initiated by OVA-C-CPE, OVA was fused with C-CPE303, resulting in OVA-C-CPE303. B) Interaction of OVA-C-CPE303 with claudin-4. Binding of OVA-C-CPE303 to claudin-4 was investigated by ELISA with wild-type BV (WT-BV), claudin-1 or -4-displaying BV (CL1-BV, CL4-BV). C) Immune responses by OVA-C-CPE303. Mice were nasally immunized with OVA, OVA-C-CPE or OVA-C-CPE303 (5 μg OVA) once a week for 3 weeks. Seven days after the last immunization, the levels of serum IgG (C), nasal IgA (D), vaginal IgA (E) and fecal IgA (F) were measured by ELISA. Data are means ± SD ($n = 4$). Data are representative of three independent experiments.